Chapter 15

NORMAN I. NORRISH AND
DUNCAN C. WYLLIE

ROCK SLOPE STABILITY ANALYSIS

1. INTRODUCTION

Except for the rare case of a completely unfractured rock unit, the majority of rock masses can be considered as assemblages of intact rock blocks delineated in three dimensions by a system of discontinuities. These discontinuities can occur as unique randomly oriented features or as repeating members of a discontinuity set. This system of structural discontinuities is usually referred to as the structural fabric of the rock mass and can consist of bedding surfaces, joints, foliation, or any other natural break in the rock. In most cases, engineering properties of fractured rock masses, such as strength, permeability, and deformability, are more dependent on the nature of the structural fabric than on the properties of the intact rock. For this reason, practitioners in the field of rock mechanics have developed the following parameters to characterize the nature of the discontinuities that make up the structural fabric:

- **Orientation:** The orientation of a discontinuity is best defined by two angular parameters: dip and dip direction.
- **Persistence:** Persistence refers to the continuity or areal extent of a discontinuity and is particularly important because it defines the potential volume of the failure mass. Persistence is difficult to quantify; the only reliable means is mapping of bedrock exposures.
- **Spacing:** The distance between two discontinuities of the same set measured normal to the discontinuity surfaces is called spacing. Together, persistence and spacing of discontinuities define the size of blocks. They also influence the dilatancy of the rock mass during shear displacement and determine the extent to which the mechanical properties of the intact rock will govern the behavior of the rock mass.
- **Surface properties:** The shape and roughness of the discontinuity constitute its surface properties, which have a direct effect on shear strength.
- **Infillings:** Minerals or other materials that occur between the intact rock walls of discontinuities are termed infillings. Their presence can affect the permeability and shear strength of a discontinuity. Secondary minerals, such as calcite or quartz, may provide significant cohesion along discontinuities. However, these thin infillings are susceptible to damage by blasting, resulting in total loss of cohesion.

For all but very weak rock materials, the analysis of rock slope stability is fundamentally a two-part process. The first step is to analyze the structural fabric of the site to determine if the orientation of the discontinuities could result in instability of the slope under consideration. This determination is usually accomplished by means of stereographic analysis of the structural fabric and is often referred to as *kinematic analysis* (Piteau and Peckover 1978). Once it has been determined that a kinematically possible failure mode is present, the second step re-

quires a limit-equilibrium stability analysis to compare the forces resisting failure with the forces causing failure. The ratio between these two sets of forces is termed the factor of safety, *FS*.

For very weak rock where the intact material strength is of the same magnitude as the induced stresses, the structural geology may not control stability, and classical soil mechanics principles for slope stability analysis apply. These procedures are discussed in Chapter 13.

2. TYPES OF ROCK SLOPE FAILURES

As shown in Figure 15-1, most rock slope failures can be classified into one of four categories depending on the type and degree of structural control:

- *Planar failures* are governed by a single discontinuity surface dipping out of a slope face [Figure 15-1(*a*)],
- *Wedge failures* involve a failure mass defined by two discontinuities with a line of intersection that is inclined out of the slope face [Figure 15-1(*b*)],
- *Toppling failures* involve slabs or columns of rock defined by discontinuities that dip steeply into the slope face [Figure 15-1(*c*)], and
- *Circular failures* occur in rock masses that are either highly fractured or composed of material with low intact strength [Figure 15-1(*d*)].

Recognition of these four categories of failures is essential to the application of appropriate analytical methods.

3. STEREOGRAPHIC ANALYSIS OF STRUCTURAL FABRIC

From a rock slope design perspective, the most important characteristic of a discontinuity is its

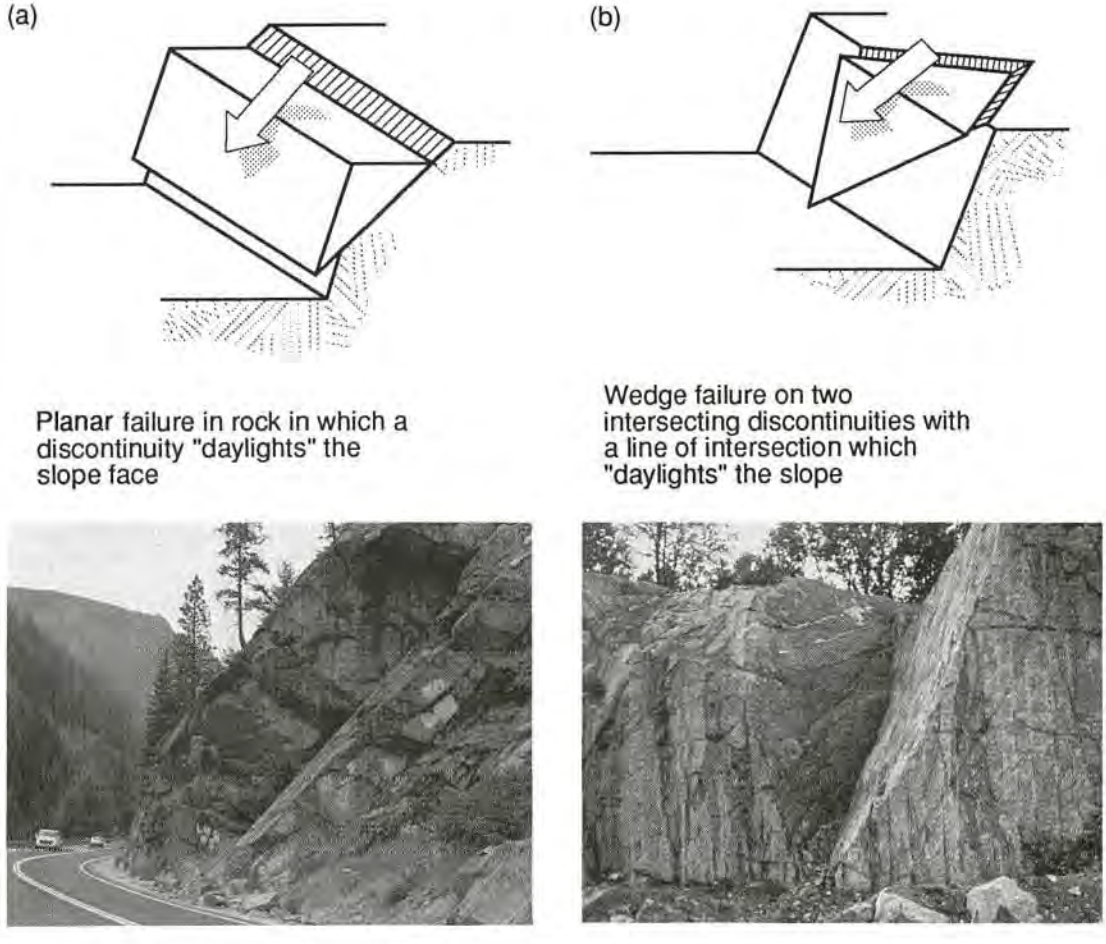

FIGURE 15-1 *(facing pages)* Types of rock slope failures: (*a*) planar failure, (*b*) wedge failure, (*c*) toppling failure, (*d*) circular failure (diagrams modified from Hoek and Bray 1981).
N.I. NORRISH AND D.C. WYLLIE

orientation, which is best defined by two parameters: dip and dip direction [Figure 15-2(*a*)]. The dip angle refers to the inclination of the plane below the horizontal and thus ranges from 0 to 90 degrees. The dip direction of the plane is the azimuth at which the maximum dip is measured and ranges from 0 to 360 degrees. The dip direction differs from the strike direction by 90 degrees and is the preferred parameter to avoid ambiguity as to the direction of dip. These values are determined by compass measurements on rock outcrops (Chapter 9), oriented drilling techniques, or interpretation of geologic structural trends (Chapter 8).

Interpretation of these geologic structural data requires the use of stereographic projections that allow the three-dimensional orientation data to be represented and analyzed in two dimensions. The most commonly used projections are the equal-area net and the polar net, replications of which are shown in Appendix A.

The rock slope practitioner is referred to the work by Hoek and Bray (1981), Hoek and Brown (1980), and Goodman (1976) for in-depth treatment of the principles of stereographic analysis. A detailed presentation of the procedures for plotting, analyzing, and interpreting data on stereographic projections is beyond the scope of this report; however, these techniques are essential to rock slope design and to the following discussion.

Stereographic presentations remove one dimension from consideration so that planes can be represented by lines and lines represented by points. Stereographic analyses consider only angular relationships between lines, planes, and lines and planes. These analyses do not in any way represent the position or size of the feature.

The fundamental concept of stereographic projections consists of a reference sphere that has a fixed orientation of its axis relative to the north and of its equatorial plane to the horizontal [Figure

(c)

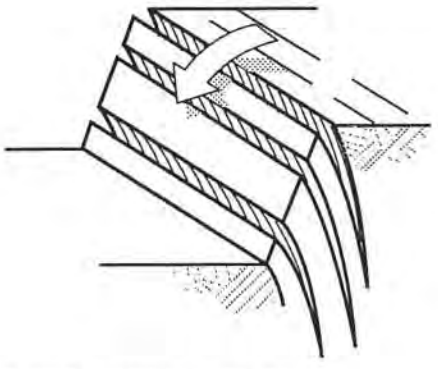

Toppling failure in hard rock with slabs or columns defined by discontinuities that dip steeply into the slope

(d)

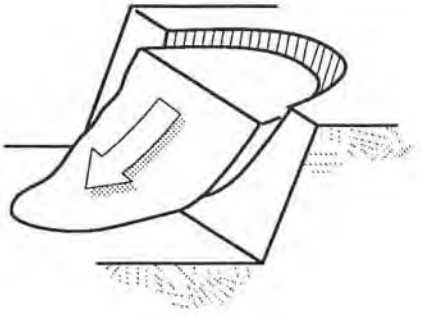

Circular failure in overburden soil, waste rock or heavily fractured rock with no identifiable structural pattern

FIGURE 15-2 Concepts for stereographic representation of linear and planar features (modified from Hoek and Bray 1981).

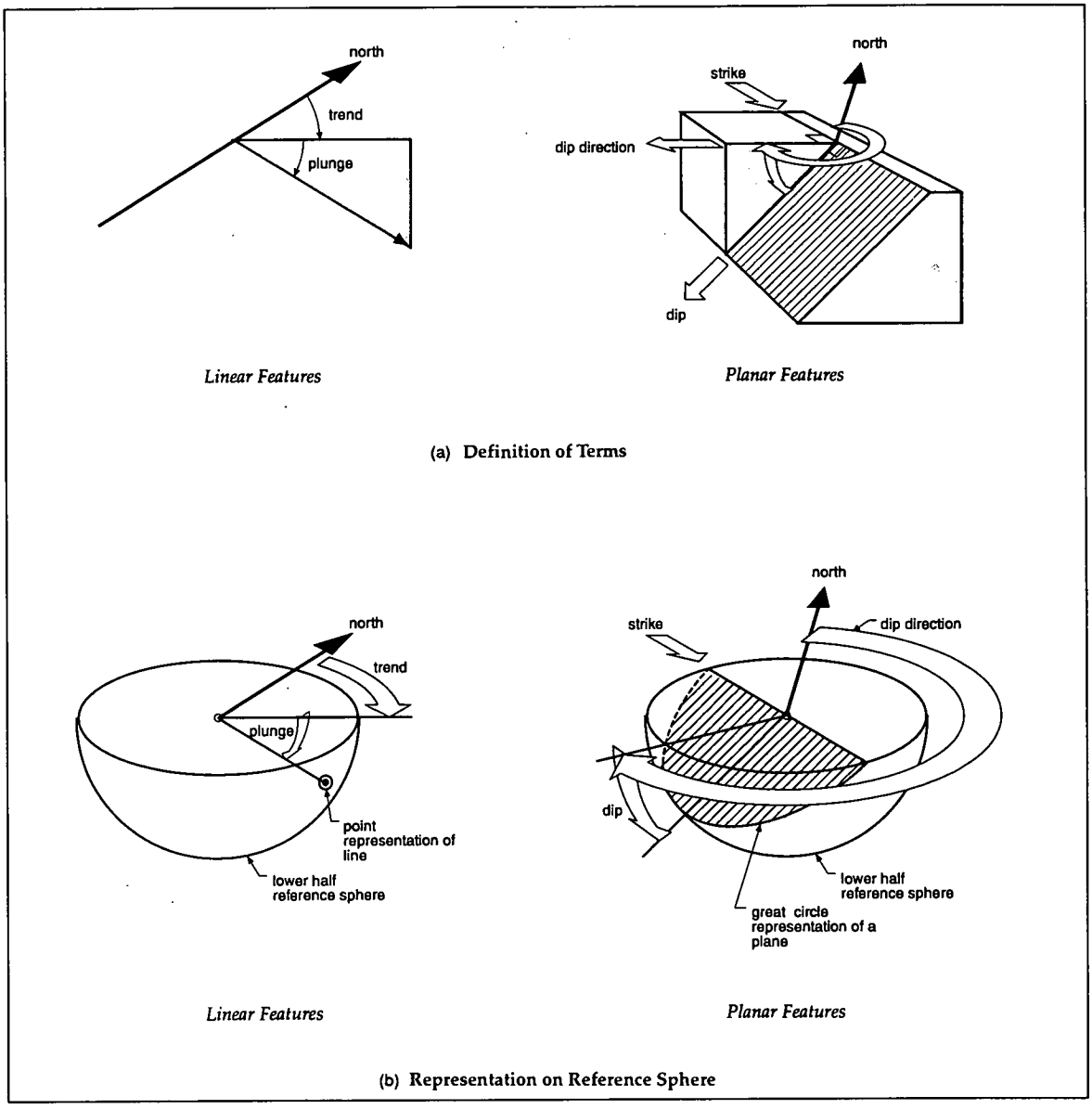

15-2(*b*)]. Linear features with a specific plunge and trend are positioned in an imaginary sense so that the axis of the feature passes through the center of the reference sphere. The intersection of the linear feature with the lower half of the reference sphere defines a unique point [Figure 15-3(*a*)]. Depending on the type of stereographic projection, this point is rotated down to a unique point on the stereonet. For the purposes of this discussion, only equal-area nets will be considered, although the reader should be aware that equal-angle projections can also be used. Linear features with shallow plunges plot near the circumference of the stereographic projection, whereas those with steep plunges plot near the center. Similarly, planar features are positioned so that the feature passes through the center of the reference sphere and produces a unique intersection line with the lower half of the reference sphere [Figures 15-2(*b*) and 15-3(*b*)]. The projection of this intersection line onto the stereographic plot results in a unique representation of that plane referred to as a *great circle*. Planes with shallow dips have great circles that plot near the circumference of the net, and those with steep dips plot near the center. Planes are used to represent both discontinuities and slope faces in stereographic analyses.

A useful alternative method of representing planes is to use the normal to the plane. This nor-

mal in a stereographic projection will be a unique point that is referred to as the *pole to the plane* [Figure 15-3(*b*)]. Structural mapping data of discontinuities are often plotted in the pole format rather than the great-circle format in order to detect the presence of preferred orientations, thus defining discontinuity sets, and to determine mean and extreme values for the orientations of these sets. As shown in Figure 15-4, this process can be facilitated by contouring to accentuate and distinguish the repetitive features from the random or unique features. Computerized graphical methods greatly facilitate the analysis of large amounts of structural data. However, when fewer than 50 data points are involved, manual plotting and analysis are probably more efficient.

The intersection of two planes defines a line in space that is characterized by a trend (0 to 360 degrees) and plunge (0 to 90 degrees). In stereographic projection, this line of intersection is defined at the point where the two great circles cross, and the trend and plunge of this point are determined by conventional stereographic principles. It is interesting to note that the line of intersection, represented by a point on a stereonet, is the pole to a great circle containing the poles of the two wedge-forming discontinuities.

4. PLANAR FAILURE

Planar failures are those in which movement occurs by sliding on a single discrete surface that approximates a plane [Figure 15-1(*a*)]. Planar failures are analyzed as two-dimensional problems. Additional discontinuities may define the lateral extent of planar failures, but these surfaces are considered to be release surfaces, which do not contribute to the stability of the failure mass. Alternatively, the planar failure may be located on a nose of rock so that the slope forms the lateral termination of the failure mass.

The size of planar failures can range from a few cubic meters to large-scale landslides that involve entire mountainsides. The K M Mountain landslide in the state of Washington (Lowell 1990), which involved an estimated 1.2 to 1.5 million m^3, was controlled by the bedding orientation within a siltstone sequence. The 1965 Hope landslide in southern British Columbia occurred along planar felsite dikes dipping subparallel to the slope and involved approximately 48 million m^3 of displaced material (Mathews and McTaggert 1969).

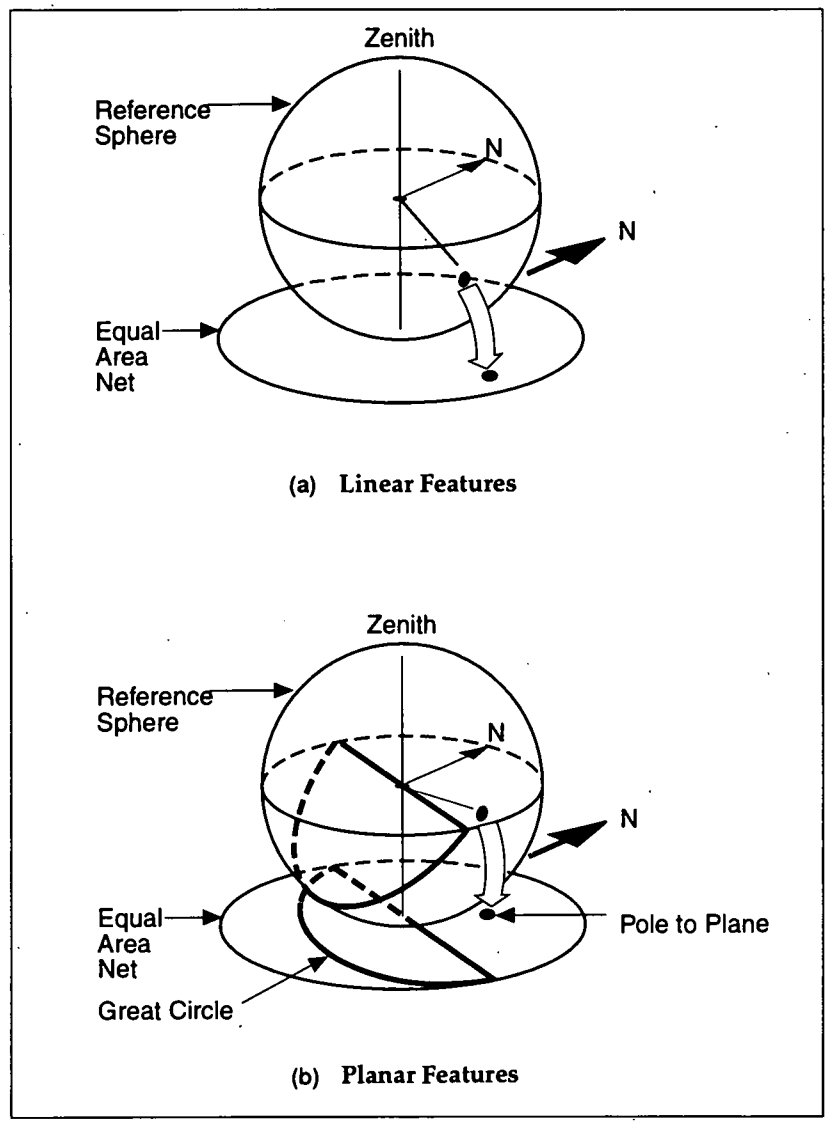

FIGURE 15-3 Equal-area projections for linear and planar features (modified from Hoek and Bray 1981).

4.1 Kinematic Analysis

The four necessary structural conditions for planar failures can be summarized as follows:

1. The dip direction of the planar discontinuity must be within 20 degrees of the dip direction of the slope face, or, stated in a different way, the strike of the planar discontinuity must be within 20 degrees of the strike of the slope face.
2. The dip of the planar discontinuity must be less than the dip of the slope face and thereby must "daylight" in the slope face.
3. The dip of the planar discontinuity must be greater than the angle of friction of the surface.
4. The lateral extent of the potential failure mass

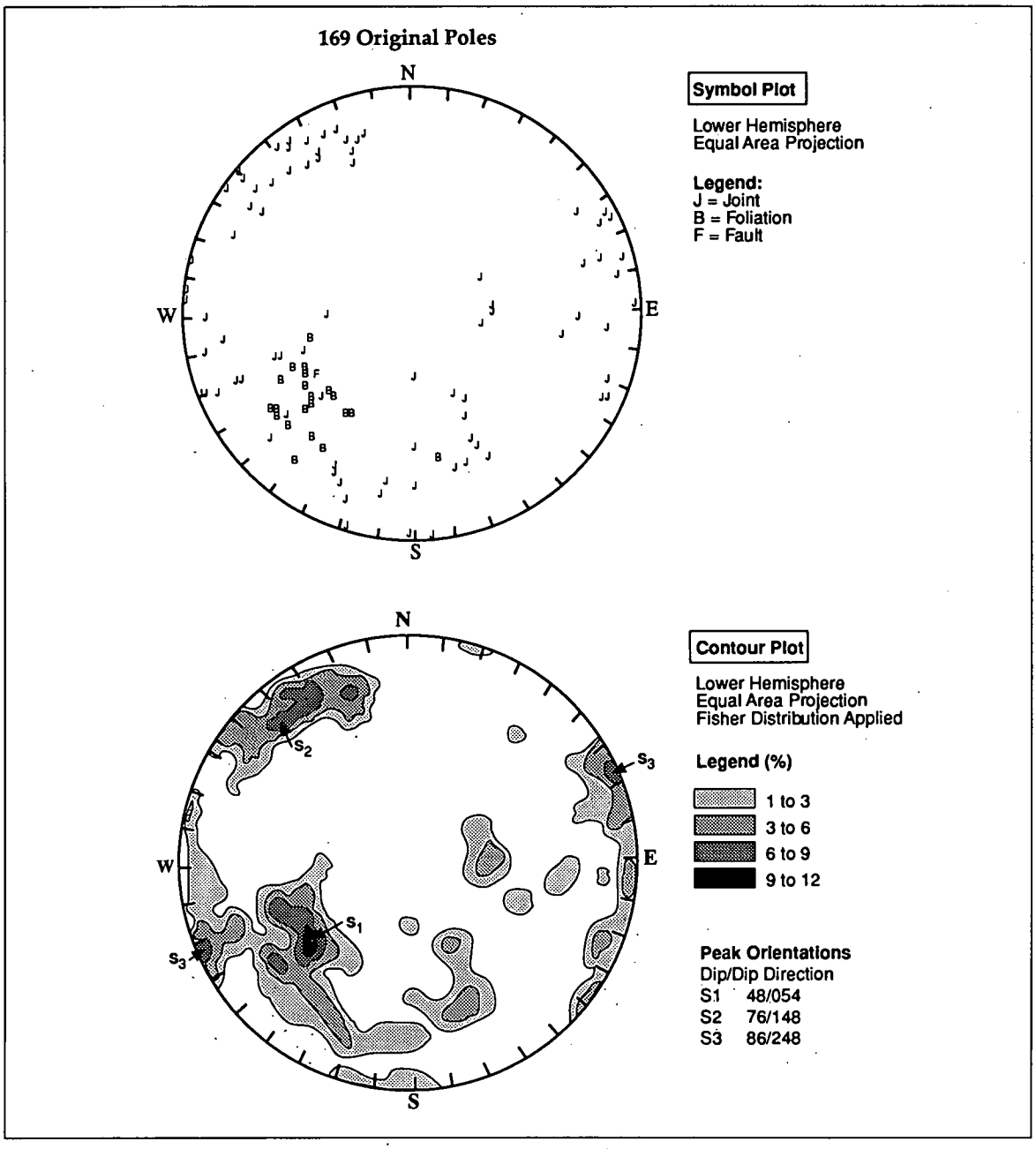

FIGURE 15-4 Examples of symbol and contour plots of pole projections in equal-area stereographic projections.

must be defined either by lateral release surfaces that do not contribute to the stability of the mass or by the presence of a convex slope shape that is intersected by the planar discontinuity.

Figure 15-5 illustrates the first three of these conditions; these are the only conditions that can be evaluated by stereographic analysis.

The presence of significant pore-water pressures along the failure surface can in some cases alter the kinematic possibility of planar failure. For example, the introduction of water pressure may cause a failure even though the dip of the failure plane is less than the frictional strength of the plane. Hodge and Freeze (1977) have presented an in-depth perspective of the influence of groundwater flow systems on the stability of interbedded sedimentary rock slopes.

4.2 Stability Analysis

If the kinematic analysis indicates that the requisite geologic structural conditions are present, stability must be evaluated by a limit-equilibrium

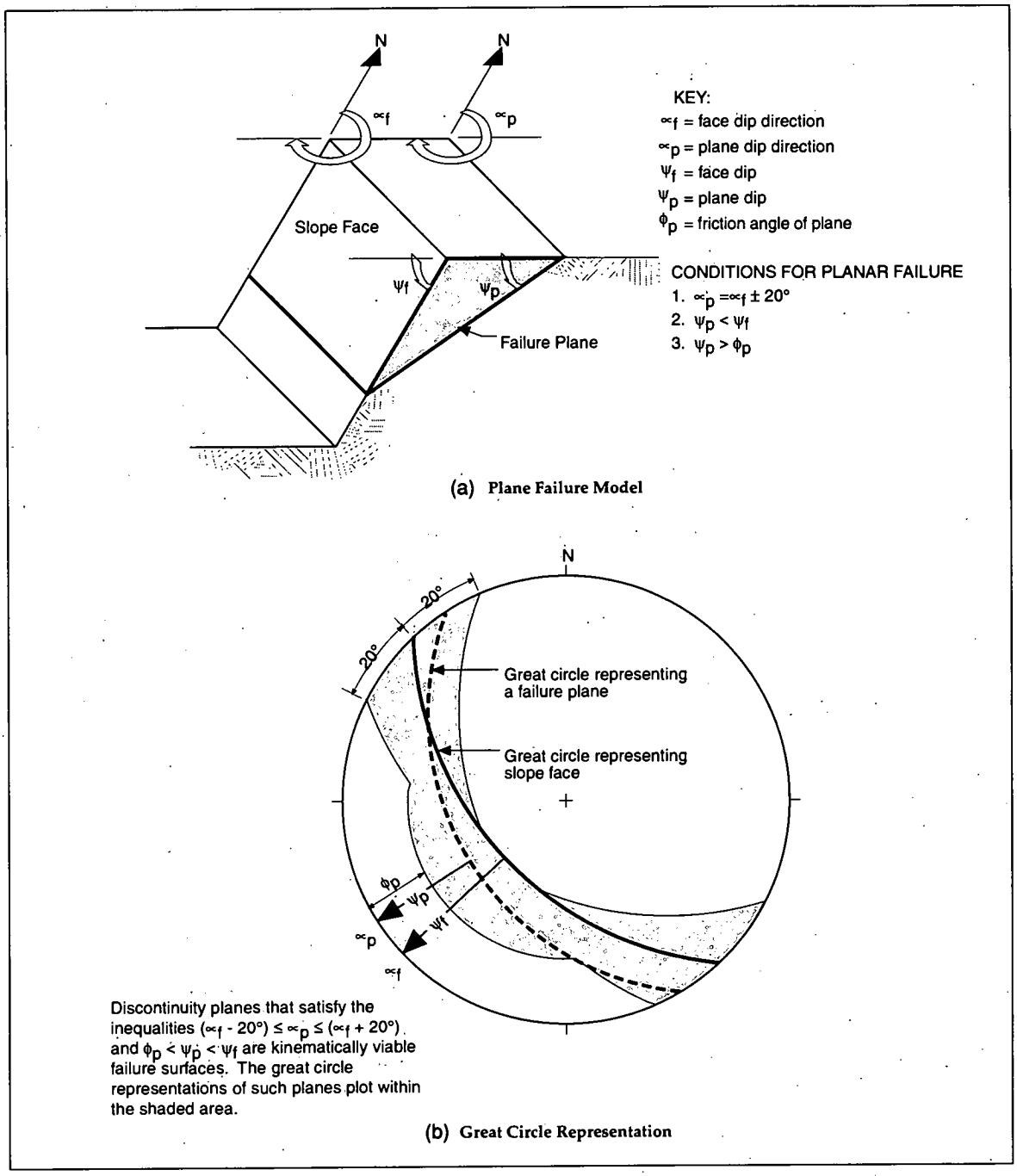

FIGURE 15-5 Kinematic analysis for planar failure.

analysis, which considers the shear strength along the failure surface, the effects of pore-water pressures, and the influence of external forces such as reinforcing elements or seismic accelerations.

Stability analysis for planar failure requires the resolution of forces perpendicular to and parallel to the potential failure surface. This resolution can be carried out in either two or three dimensions, but the most common case is the former, in which the stability formulation considers a unit thickness of the slope. Two geometric cases are considered (Figure 15-6), depending on the location of the tension crack relative to the crest of the slope:

- Tension crack present in slope face [Figure 15-6(*a*)], and
- Tension crack present in upper slope surface [Figure 15-6(*b*)].

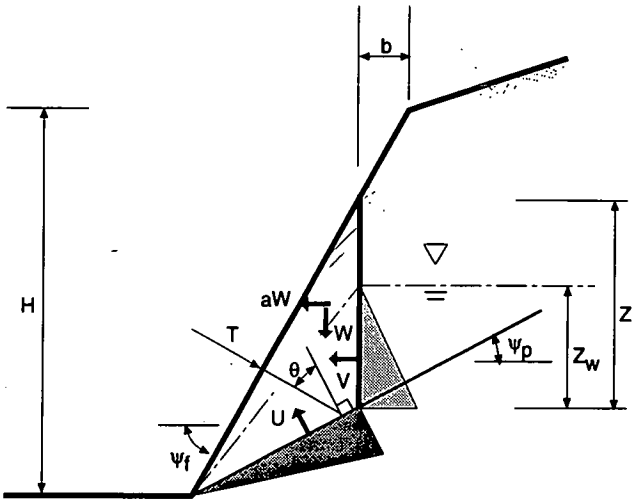

(a) Tension Crack in Slope Face

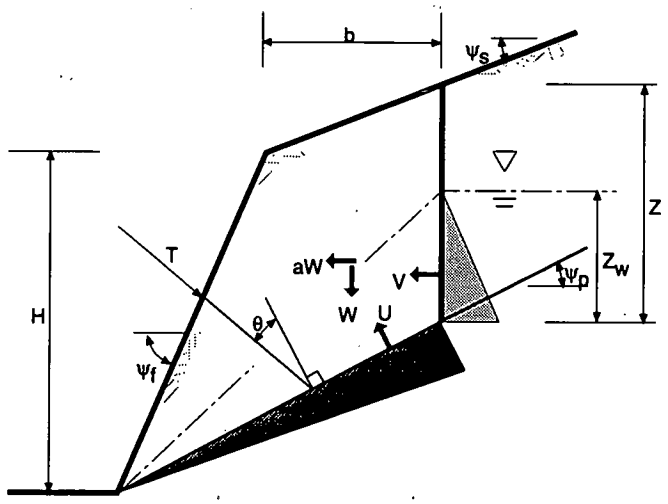

(b) Tension Crack in Upper Slope Surface

The stability equations are as follows:

For Case a:

Depth of tension crack:

$Z = (H \cot\Psi_f - b)\,(\tan\Psi_f - \tan\Psi_p)$

Weight of block:

$W = (1/2)\gamma_r H^2\,[(1 - Z/H)^2 \cot\Psi_p\,(\cot\Psi_p \tan\Psi_f - 1)]$

Area of sliding plane:

$A = (H \cot\Psi_f - b)\sec\Psi_p$

For Case b:

Depth of tension crack:

$Z = H + b\tan\Psi_s - (b + H\cot\Psi_f)\tan\Psi_p$

Weight of block:

$W = (1/2)\gamma_r (H^2 \cot\Psi_f X + bHX + bZ)$

$X = (1 - \tan\Psi_p \cot\Psi_f)$

Area of sliding plane:

$A = (H \cot\Psi_f + b)\sec\Psi_p$

For either Case a or b:

Uplift water force:

$U = (1/2)\gamma_w Z_w A$

Driving water force:

$V = (1/2)\gamma_w Z_w^2$

Factor of safety:

$$FS = \frac{\{cA + [W(\cos\Psi_p - a\sin\Psi_p) - U - V\sin\Psi_p + T\cos\theta]\tan\phi\}}{[W(\sin\Psi_p + a\cos\Psi_p) + V\cos\Psi_p - T\sin\theta]}$$

where

H = height of slope face;
Ψ_f = inclination of slope face;
Ψ_s = inclination of upper slope face;
Ψ_p = inclination of failure plane;
b = distance of tension crack from slope crest;
a = horizontal acceleration, blast or earthquake loading;
T = tension in bolts or cables;
θ = inclination of bolt or cable to normal to failure plane;
c = cohesive strength of failure surface;
ϕ = friction angle of failure surface;
γ_r = density of rock;
γ_w = density of water;
Z_w = height of water in tension crack;
Z = depth of tension crack;
U = uplift water force;
V = driving water force;
W = weight of sliding block; and
A = area of failure surface.

A simplified groundwater model consists of a measured depth of water in the tension crack defining a phreatic surface that is assumed to decrease linearly toward and exit at the toe of the slope. Other configurations of the phreatic surface can be assumed with consequent modification to the forces U and V (Figure 15-6). The stability equations also incorporate external stabilizing forces, for example, those due to bolts or cables, and destabilizing forces such as those due to seismic ground accelerations.

Of particular note in Figure 15-6 is the location of the tension crack, expressed by the di-

mension b. In most cases, small-magnitude antecedent movements will define the location of the tension crack so that the geometry for slope analysis can be ascertained. However, in some cases these movements may not have occurred or the tension crack may be covered with surficial soils. In such circumstances, an approximation incorporating the most probable or "critical" tension crack location is as follows (Hoek and Bray 1981):

$$b/H = \sqrt{(\cot\Psi_f \cot\Psi_p)} - \cot\Psi_f \qquad (15.1)$$

The derivation of this equation assumes a dry slope and a horizontal upper slope surface, but as a first approximation, it is probably adequate for most cases. Sensitivity analyses should be carried out when the geometric or other parameters are not well defined.

For either of the two cases shown in Figure 15-6, the factor of safety, FS, is expressed as shown in the box below:

$$FS = \frac{\{cA + [W(\cos\Psi_p - a\sin\Psi_p) - U - V\sin\Psi_p + T\cos\theta]\tan\phi\}}{[W(\sin\Psi_p + a\cos\Psi_p) + V\cos\Psi_p - T\sin\theta]} \qquad (15.2)$$

This expression can be simplified in a number of successive cases as follows:

External forces not present ($a = T = 0$):

$$FS = \frac{[cA + (W\cos\Psi_p - U - V\sin\Psi_p)\tan\phi]}{(W\sin\Psi_p + V\cos\Psi_p)} \qquad (15.3)$$

Dry slope ($U = V = 0$) and external forces not present ($a = T = 0$):

$$FS = \frac{(cA + W\cos\Psi_p\tan\phi)}{(W\sin\Psi_p)} \qquad (15.4)$$

Cohesionless surface ($c = 0$), dry slope ($U = V = 0$), and external forces not present ($a = T = 0$):

$$FS = \frac{(\tan\phi)}{(\tan\Psi_p)} \qquad (15.5)$$

In this simplest case, the factor of safety for the slope is unity when the inclination of the failure surface equals the angle of friction for the surface. This relationship forms the basis of tilt tests, which are used to estimate base friction angles using blocks of rock or intact pieces of core (Franklin and Dusseault 1989).

Alternative methods of stability analysis for planar failures include limit-equilibrium analyses, which incorporate the method of slices to approximate the slope and failure-surface geometry. As an example, Sarma (1979) presented a method that can be applied to both circular and noncircular sliding surfaces. Hoek and Bray (1981) developed graphical solutions for planar failures for the case in which the external forces are zero and the upper slope surface is horizontal.

FIGURE 15-6 *(opposite page)* Two geometric cases of planar failure (modified from Hoek and Bray 1981).

4.3 Case Example of Planar Failure

Methods of stability analysis for planar failures can be best explained by the use of a case example.

4.3.1 Problem Description

Structural mapping of an existing highway cut reveals the existence of well-developed foliation with a mean orientation of 30 degrees/145 degrees (dip/dip direction). The slope face is 30 m high with an orientation of 70 degrees/135 degrees. Further examination of the 11-degree upper slope indicates the presence of a tension crack 15 m behind the slope crest with water in the tension crack 9 m deep, as shown in Figure 15-7(a). Because of infilling and roughness along the foliation planes, the surfaces are characterized by shear strength parameters that include a friction angle of 25 degrees and a cohesion of 96 kPa. The rock mass is estimated to have a unit weight of 25 kN/m^3. The slope designer is required to perform analyses to demonstrate the existing factor of safety. If this evaluation indicates a factor of safety less than 1.5, a slope-stabilization program must be designed to provide this value. The sensitivity of the slope stability to groundwater fluctuations and to seismic accelerations must also be determined.

4.3.2 Solution

A stereographic analysis of the slope and discontinuity orientations indicates that the three conditions necessary for a kinematically possible failure surface are present [Figure 15-7(b)]:

- The dip direction of the foliation and that of the slope face are within 20 degrees,

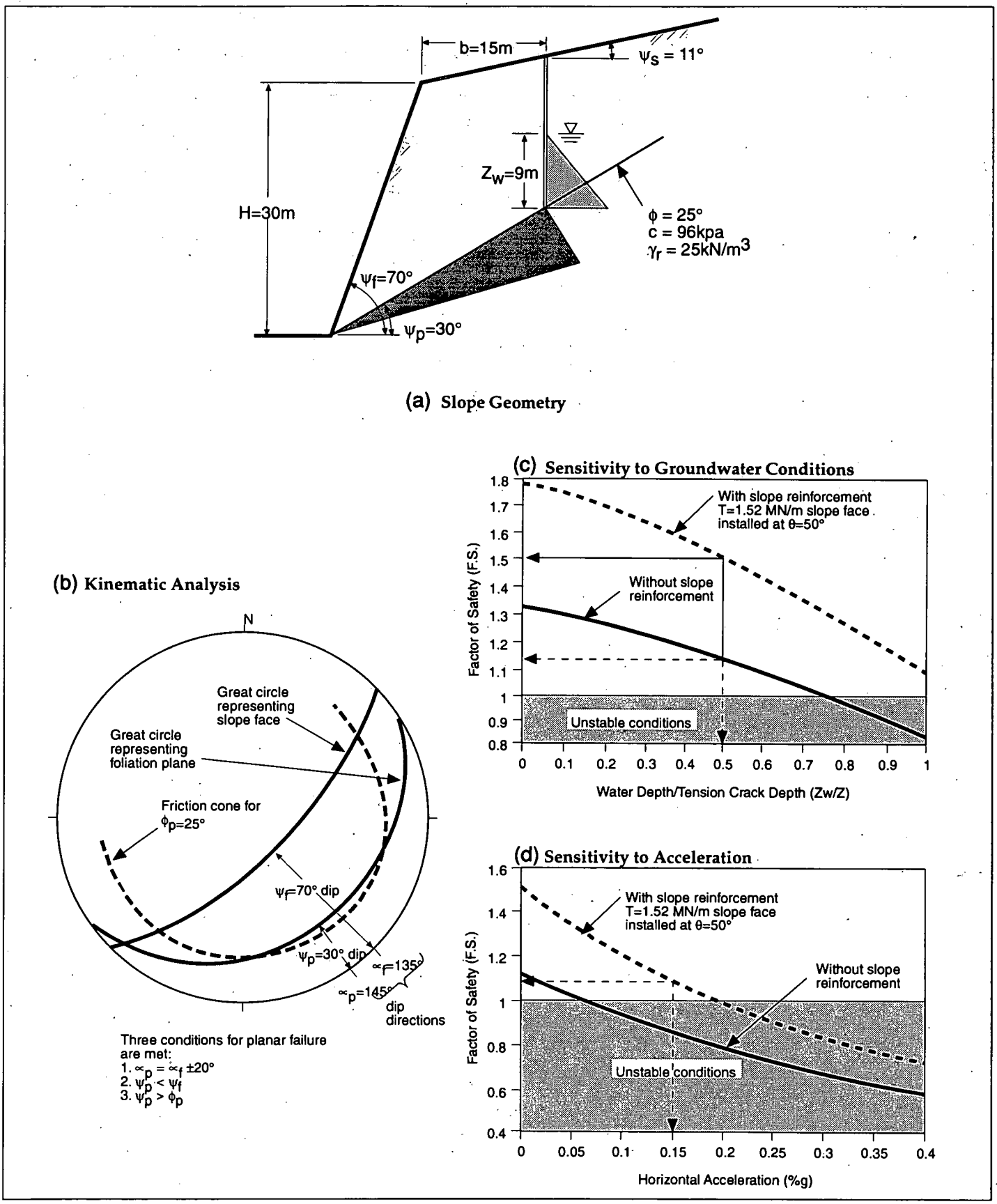

FIGURE 15-7
Case example of planar failure.

- The dip of the foliation is less than the dip of the slope face, and
- The dip of the foliation exceeds its angle of friction.

Having determined that a planar failure is possible, the next step is to determine the degree of stability (or instability) by calculating the factor of safety. Evaluation of the stability of the slope requires the solution of the equations represented by Figure 15-6(*b*). The computations are shown in the box below.

tions given in Section 4.2 into a commercially available spreadsheet program that enables the development of stability graphs such as those in Figure 15-7(*c*) and (*d*). As an example, to examine the feasibility of stabilization through slope drainage, the accompanying sensitivity graph [Figure 15-7(*c*)] demonstrates that the factor of safety ranges from a high of 1.32 for a dry slope to a low of 0.82 for a fully saturated, unreinforced slope. Even if measures to promote permanent drainage of the slope were implemented, a factor of safety of 1.32 would probably be marginal (in

Depth of tension crack:

$Z = 30 + 15(\tan 11°) - [15 + 30(\cot 70°)] \tan 30°$
$= 18$ m

Weight of block:

$W = \frac{25}{2}[(30)^2 \cot 70° (X) + (15)(30)(X) + (15)(18)]$

where

$X = (1 - \tan 30° \cot 70°) = 0.79$

then

$W = 11.05$ MN/m

Area of sliding plane:

$A = (30 \cot 70° + 15)(\sec 30°) = 29.9$ m²/m

Uplift water force:

$U = (1/2)(10)(9)(29.9) = 1.35$ MN/m

Driving water force:

$V = (1/2)(10)(9)^2 = 0.41$ MN/m

Substituting these values into Equation 15.3 for the case where external forces are not present yields

$$FS = \frac{\{(0.096)(29.9) + [(11.05)(\cos 30°) - 1.35 - (0.41)(\sin 30°)] (\tan 25°)\}}{[(11.05)(\sin 30° + (0.41)(\cos 30°)]}$$

$FS = 6.61/5.88 = 1.12$

The calculated factor of safety for the existing condition is 1.12, which corresponds to a tension crack half-filled with water ($Z_w/Z = 0.5$). This factor of safety would be considered unacceptable for the long-term performance of the slope, and therefore stabilization should be undertaken.

To analyze stabilization alternatives, it is useful to perform sensitivity analyses that illustrate the dependence of slope stability on various parameters of interest. These analyses are most easily accomplished by programming the stability equa-

most design circumstances), and other stabilization methods should be considered.

Equation 15.2 can be used to calculate the bolting force, T, necessary to provide the required factor of safety of 1.5. For illustrative purposes, the inclination of the bolting force will be set at $\theta = 50$ degrees. Although this is not the optimal orientation, practical considerations would dictate that the anchor holes be drilled below horizontal to facilitate grouting. Substituting these values into Equation 15.2 produces the computations below:

$$1.5 = \frac{\{(0.096)(29.9) + [(11.05)(\cos 30°) - 1.35 - (0.41)(\sin 30°) + T(\cos 50°)](\tan 25°)\}}{(11.05)[\sin 30° + (0.41)(\cos 30°) - T(\sin 50°)]}$$

$$1.5 = \frac{[2.87 + (8.01 + 0.64T)(\tan 25°)]}{(5.88 - 0.77T)}$$

$T = 1.52$ MN/m

It is important to note that T is computed in terms of the force per unit of slope length. This value combined with the selected bolt or anchor capacity defines the required bolt spacing. The slope designer should verify that the reinforced slope will be stable under the saturated slope extreme ($Z_w/Z = 1$). For the case example, the sensitivity analysis in Figure 15-7(*c*) indicates an acceptable factor of safety of 1.08 under this condition.

The stability of the reinforced slope for a design horizontal acceleration, $a = 0.15g$, is verified using Equation 15.2 according to the computation shown in the box below.

The variation of stability of the reinforced slope with seismic acceleration is shown in the sensitivity graph of Figure 15-7(*d*). For the case example, a factor of safety of 1.5 under static conditions with a corresponding factor of safety of 1.09 for a design acceleration of 0.15*g* would generally be considered prudent engineering practice. Figure 15-7(*d*) also indicates a limiting acceleration equivalent to 0.19*g* for the reinforced slope.

$$FS = \frac{\{(0.096)(29.9) + [(11.05)(\cos 30°) - (0.15)(\sin 30°) - 1.35 - (0.41)(\sin 30°) + (1.52)(\cos 50°)](\tan 25°)\}}{(11.05)[\sin 30° + (0.15)(\cos 30°) + (0.41)(\cos 30°) - (1.52)(\sin 50°)]}$$

$$FS = 6.68/6.15 = 1.09$$

FIGURE 15-8 Massive wedge failure along I-40 in mountainous sections of eastern Tennessee that closed two lanes for more than two weeks (Moore 1986).

5. WEDGE FAILURE

Wedge failures result when rock masses slide along two intersecting discontinuities both of which dip out of the cut slope at an oblique angle to the cut face, forming a wedge-shaped block [Figures 15-1(*b*) and 15-8]. Commonly, these rock wedges are exposed by excavations that daylight the line of intersection that forms the axis of sliding, precipitating movement of the rock mass either along both planes simultaneously or along the steeper of the two planes in the direction of maximum dip.

Depending upon the ratio between peak and residual shear strengths, wedge failures can occur rapidly, within seconds or minutes, or over a much longer time frame, on the order of several months. The size of a wedge failure can range from a few cubic meters to very large slides from which the potential for destruction can be enormous (Figure 15-8). Figure 15-9 illustrates schematically the development of a classic wedge failure. Figure 15-9(*a*) shows a typical rock cut along a highway in which the geologic structure is conducive to wedge failure, resulting in an unstable slope condition. Incipient development of the wedge, defined by intersecting planes of fracture, cleavage, bedding, or all three, results in the formation of a V-shaped wedge of unstable rock with fully developed failure scarps, as shown in Figure 15-9(*b*). Figure 15-9(*c*) shows the rapid movement of the rock wedge failure, and its aftermath is shown in Figure 15-9(*d*).

The formation and occurrence of wedge failures are dependent primarily on lithology and structure of the rock mass (Piteau 1972). Rock masses with well-defined orthogonal joint sets or cleavages in

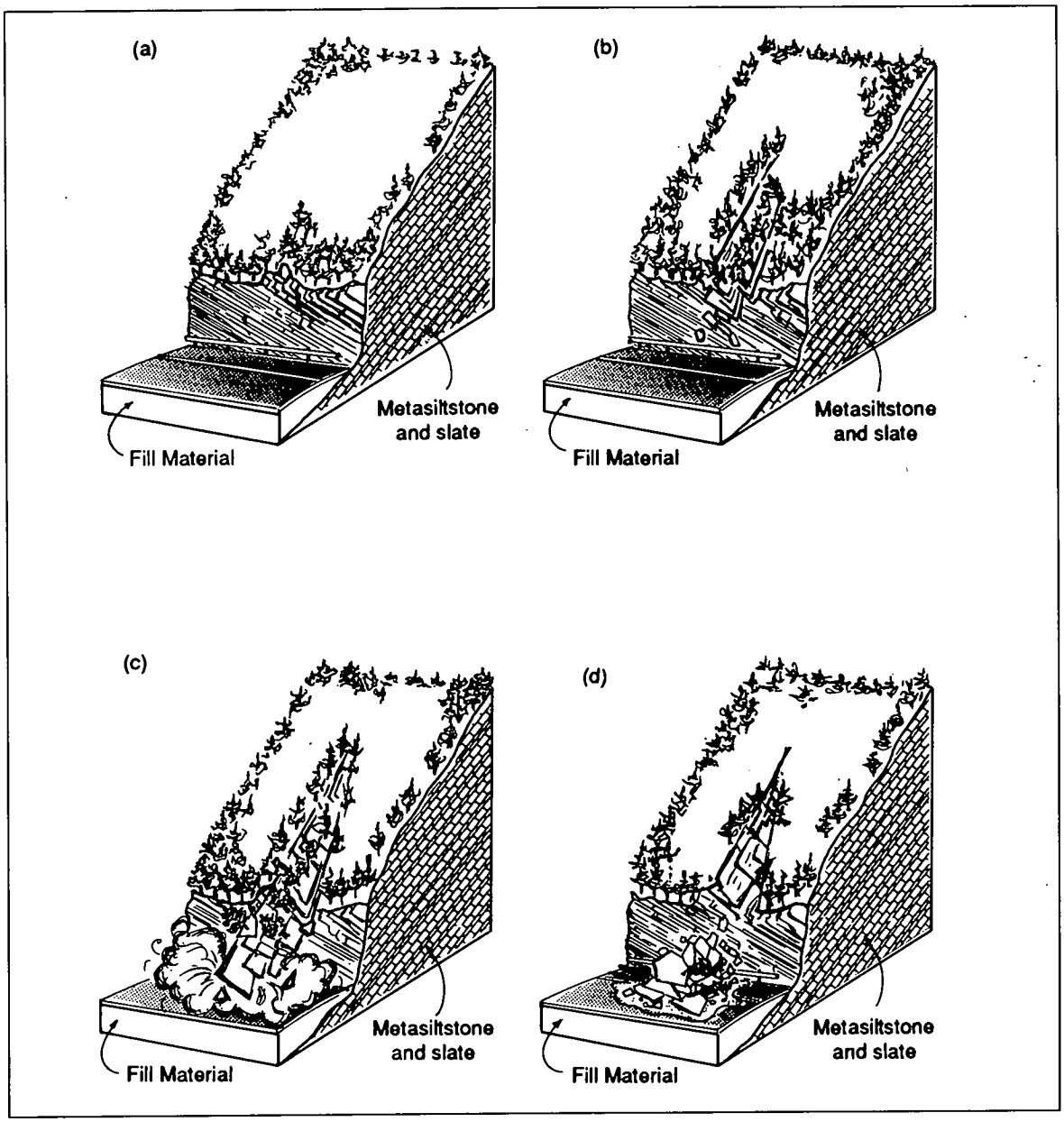

FIGURE 15-9 Stages in development of wedge-failure landslide: (*a*) rock slope as constructed; (*b*) incipient wedge failure; (*c*) rock wedge during failure; (*d*) rock slope after wedge failure (modified from Moore 1986).

addition to inclined bedding or foliation generally are favorable situations for wedge failure (Figure 15-10). Shale, thin-bedded siltstones, claystones, limestones, and slaty lithologies tend to be more prone to wedge failure development than other rock types. However, lithology alone does not control development of wedge failures.

5.1 Kinematic Analysis

A kinematic analysis for wedge failure is governed by the orientation of the line of intersection of the wedge-forming planes. Kinematic analyses determine whether sliding can occur and, if so, whether it will occur on only one of the planes or simultaneously on both planes, with movement in the direction of the line of intersection.

The necessary structural conditions for wedge failure are illustrated in Figure 15-11(*a*) and can be summarized as follows:

1. The trend of the line of intersection must approximate the dip direction of the slope face.
2. The plunge of the line of intersection must be less than the dip of the slope face. Under this

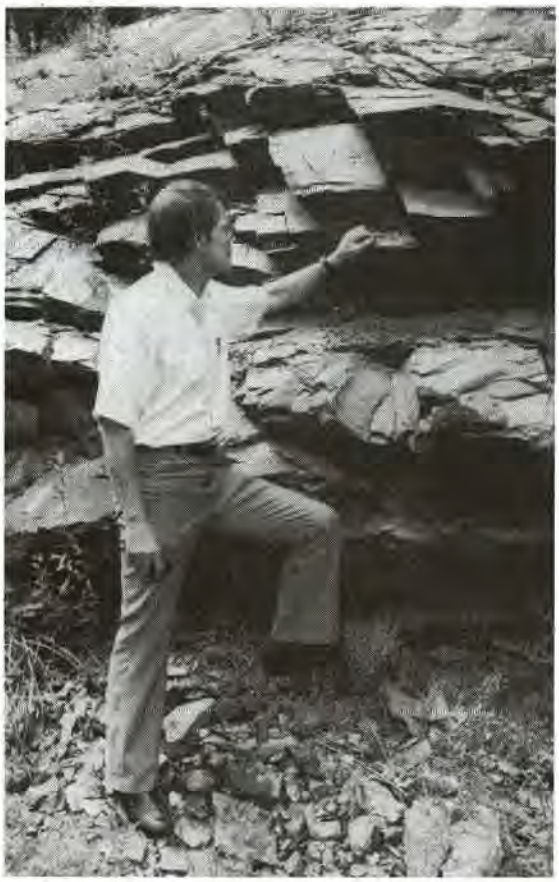

FIGURE 15-10 Exposed rock face exhibiting well-developed intersecting discontinuities with potential for wedge failure (Moore 1986.)

condition, the line of intersection is said to daylight on the slope.

3. The plunge of the line of intersection must be greater than the angle of friction of the surface. If the angles of friction for the two planes are markedly different, an average angle of friction is applicable. This condition is also shown in Figure 15-11(*a*).

Because the model represents a three-dimensional shape, no assumptions of the lateral extent of the wedge are required. Stereographic analysis can also determine whether sliding will occur on both the wedge-forming planes or on only one of the two. This procedure is referred to as Markland's test (Hoek and Bray 1981), which is described in Figure 15-11(*a*).

The presence of significant pore-water pressures along the failure planes can in some cases alter the possibility of kinematic wedge failures. For example, the introduction of water pressure may cause a failure even though the plunge of the intersection line is less than the average frictional strength of the planes.

5.2 Stability Analysis

Once a kinematic analysis of wedge stability using stereographic methods [Figure 15-11(*b*)] has been performed indicating the possibility of a wedge failure, more detailed stability analyses may be required for the design of stabilization measures. The common analytical technique is a rigid-block analysis in which failure is assumed to be by linear sliding along the line of intersection formed by the discontinuities or by sliding along one of the discontinuities. Toppling or rotational sliding is not considered in the analysis.

The analysis of wedge stability requires that the geometry of the wedge be defined by the location and orientation of as many as five bounding surfaces. These include the two intersecting discontinuities, the slope face, the upper slope surface, and, if present, the plane representing a tension crack [Figure 15-12(*a*)]. The size of the wedge is defined by the vertical distance from the crest of the slope to the line of intersection of the wedge-forming discontinuities. If a tension crack is present, the location of this bounding plane relative to the slope crest must be specified to analyze the wedge size.

The stability of the wedge can be evaluated using the factor-of-safety concept by resolving the forces acting normal to the discontinuities and in the direction parallel to the line of intersection. These forces include the weight of the wedge, external forces such as foundation loads, seismic accelerations, tensioned reinforcing elements, forces generated by water pressures acting on the surfaces, and the shear strength developed along the sliding plane or planes.

The completely general formulation of wedge stability calculation requires adherence to a strict system of notation. Hoek and Bray (1981) presented the equations for the general analysis as well as a methodology to undertake the calculation in a systematic manner. Because the calculation is extended, this general analysis is best adapted to computer solution. However, in most cases, assumptions can be made that significantly simplify the controlling stability equations so that simple calculator or graphical methods can provide a good indication of the sensitivity of the wedge stability to alternative strength and load combinations. Figure 15-12 (*a-e*) defines the calculation of wedge stability under various simplifying assumptions.

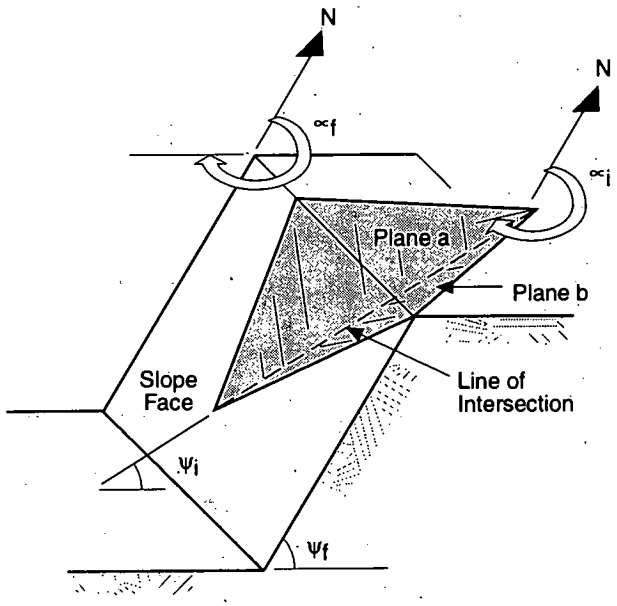

KEY:

$\propto_f$ = dip direction of face
$\propto_a$ = dip direction of plane a
$\propto_b$ = dip direction of plane b
ψ_f = dip of face
ψ_a = dip of plane a
ψ_b = dip of plane b
ϕ = friction angle
ψ_i = plunge of intersection
$\propto_i$ = azimuth of intersection

CONDITIONS FOR WEDGE FAILURE

1. $\propto_i = \propto_f \pm$ (to daylight slope face)
2. $\psi_i < \psi_f$
3. $\phi < \psi_i$

MARKLAND'S TEST

If $\propto_a$ or $\propto_b$ is between $\propto_i$ and $\propto_f$ then sliding will occur on the steeper of planes a and b in the direction of maximum dip; otherwise sliding occurs along line of intersection.

(a) **Wedge Failure Model**

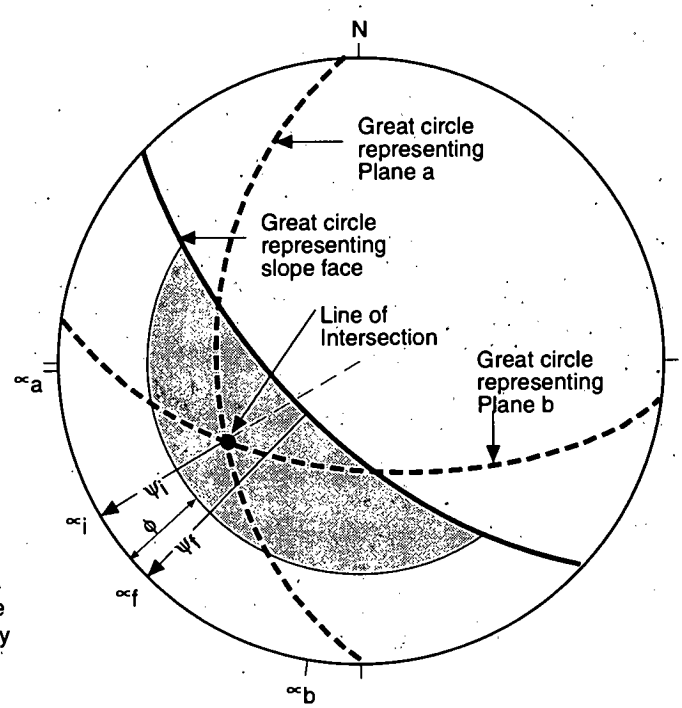

Combinations of discontinuity planes with a line of intersection that "daylights" the slope face, $\propto_i = \propto_f \pm$, and that satisfy the inequality $\phi < \psi_i < \psi_f$ represent kinematically viable wedge failures. The lines of intersection of such planes plot within the shaded area.

(b) **Great Circle Representation**

FIGURE 15-11 Kinematic analysis for wedge failure (modified from Hoek and Bray 1981).

FIGURE 15-12
(facing pages)
Stability equations for wedge failure (modified from Hoek and Bray 1981).

(a) General Case

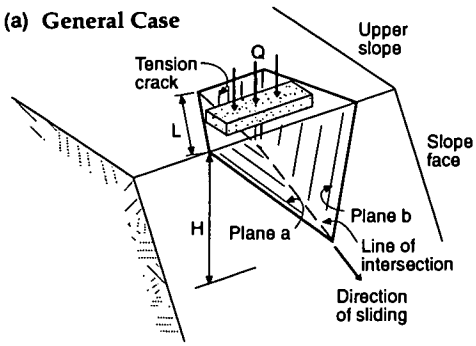

Use comprehensive solution by Hoek and Bray (1981)
Note: This solution required if external loads to be included.
Typically solved using computer program.

(b) Tension Crack Not Present

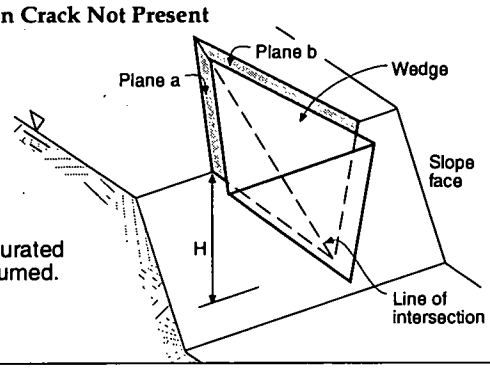

Note: Saturated slope assumed.

$$FS = \frac{3}{\gamma_r H}(c_a \bullet X + c_b \bullet Y) + (A - \frac{\gamma_w}{2\gamma_r}X)\tan\phi_a + (B - \frac{\gamma_w}{2\gamma_r}Y)\tan\phi_b$$

PARAMETERS:

c_a and c_b are the cohesive strengths of planes a and b
ϕ_a and ϕ_b are the angles of friction on planes a and b
γ_r is the unit weight of the rock
γ_w is the unit weight of water
H is the total height of the wedge
X, Y, A, and B are dimensionless factors which depend upon the geometry of the wedge
ψ_a and ψ_b are the dips of planes a and b
ψ_i is the plunge of the line of intersection

$$X = \frac{\sin\theta_{24}}{\sin\theta_{45} \bullet \mathrm{Cos}\theta_{na\bullet 2}} \qquad A = \frac{\cos\psi_a - \cos\psi_b \bullet \cos\theta_{na} \bullet nb}{\sin\psi_i \bullet \sin^2\theta_{na} \bullet nb}$$

$$Y = \frac{\sin\theta_{13}}{\sin\theta_{35} \bullet \cos\theta_{nb\bullet 1}} \qquad B = \frac{\cos\psi_b - \cos\psi_a \bullet \cos\theta_{na} \bullet nb}{\sin\psi_i \bullet \sin^2\theta_{na} \bullet nb}$$

(See Figure 15-14 for definition of angles)

(c) Fully Drained Slope

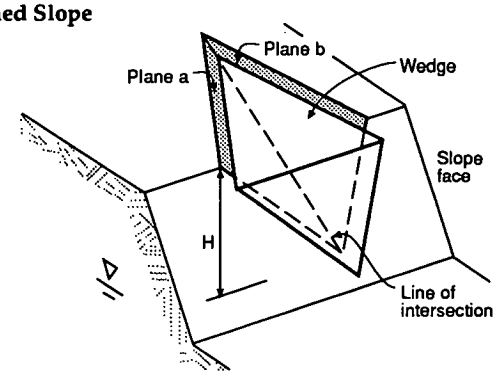

(See Figure 15-14 for definition of angles)

$$FS = \frac{3}{\gamma_r H}(c_a X + c_b Y) + A \tan \phi_a + B \tan \phi_b$$

$$X = \frac{\sin\theta_{24}}{\sin\theta_{45} \cdot \cos\theta_{na \cdot 2}}$$

$$Y = \frac{\sin\theta_{13}}{\sin\theta_{35} \cdot \cos\theta_{nb \cdot 1}}$$

$$A = \frac{\cos\psi_a - \cos\psi_b \cdot \cos\theta_{na \cdot nb}}{\sin\psi_i \cdot \sin^2\theta_{na \cdot nb}}$$

$$B = \frac{\cos\psi_b - \cos\psi_a \cdot \cos\theta_{na \cdot nb}}{\sin\psi_i \cdot \sin^2\theta_{na \cdot nb}}$$

PARAMETERS:

c_a and c_b are the cohesive strengths of planes a and b
ϕ_a and ϕ_b are the angles of friction on planes a and b
γ_r is the unit weight of the rock
H is the total height of the wedge
X, Y, A, and B are dimensionless factors which depend upon the geometry of the wedge
ψ_a and ψ_b are the dips of planes a and b
ψ_i is the plunge of the line of intersection

(d) Friction Only Shear Strengths

$$FS = A \tan \phi_a + B \tan \phi_b$$

(Parameters as above)

Note: Hoek and Bray (1981) have presented graphs to determine factors A and B.

(e) Friction Angle Same for Both Planes

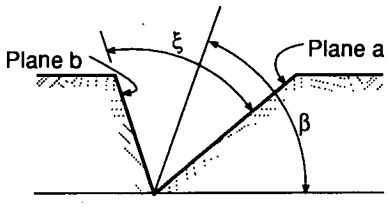

View along line of intersection

$$FS = \frac{\sin \beta}{\sin (\xi/2)} \cdot \frac{\tan \phi}{\tan \psi_i}$$

PARAMETERS:

ϕ = friction angle
ψ_i = plunge of line of intersection
β = see sketch
ξ = angle between wedge - forming planes

5.3 Case Example of Wedge Failure

Structural mapping of outcrops in the vicinity of a proposed highway cut indicates the presence of five discontinuity sets as follows:

Feature	*Dip/Dip Direction*
Bedding	48 degrees/168 degrees
Joint set 1	53 degrees/331 degrees
Joint set 2	64 degrees/073 degrees
Joint set 3	42 degrees/045 degrees
Joint set 4	45 degrees/265 degrees

The proposed cut is to be excavated at 0.25H:1V (dip of 76 degrees) with a dip direction of 196 degrees. It is estimated that the average angle of friction of the discontinuities is 30 degrees subject to confirmation by subsequent direct-shear testing.

A kinematic analysis of these data is shown in Figure 15-13. The shaded area is formed by the great circle representing the cut slope face and the friction circle for ϕ = 30 degrees. As previously shown in Figure 15-11, the lines of intersection of kinematically possible wedges plot as points within this shaded area. For the case example, Figure 15-13 shows that the intersection of the great circles representing bedding and joint set 2 (B-J2) and the intersection of the great circles representing bedding and joint set 4 (B-J4) plot

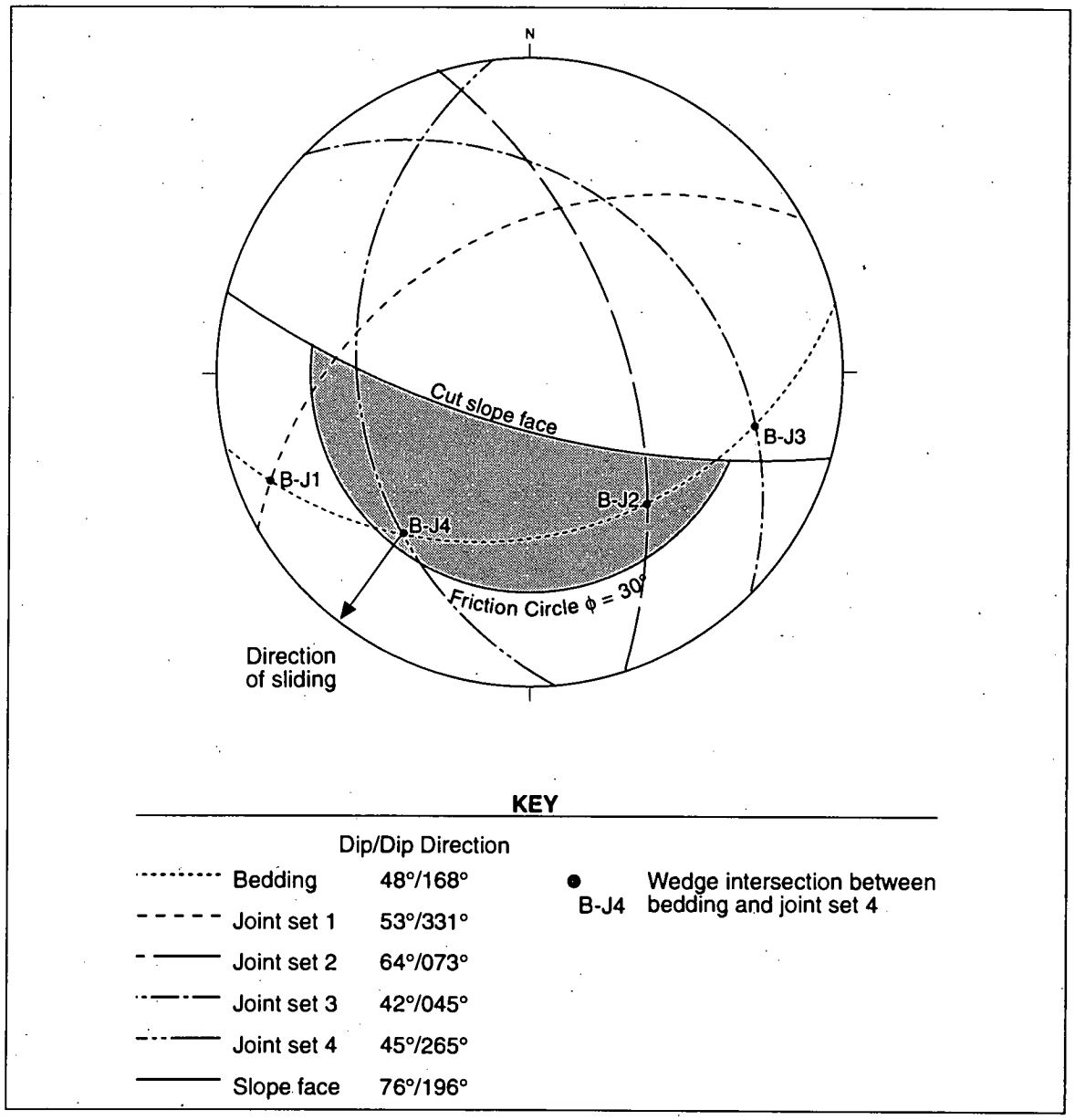

FIGURE 15-13 Great circle representation for case example of wedge failure.

within the shaded area and therefore form kinematically possible wedge failures.

To determine the factor of safety of the wedge formed by the intersection of bedding and joint set 4 (B-J4), the following additional information is obtained:

- Orientation of upper slope surface (based on mapping): 10 degrees/196 degrees dip/dip direction;
- Total wedge height (based on cross-section analysis): $H = 30$ m;
- Strength of plane a (Joint set 4) (based on laboratory testing): friction angle, $\phi_a = 35$ degrees; cohesion, $c_a = 20$ kPa;
- Strength of plane b (bedding) (based on laboratory testing): friction angle, $\phi_b = 25$ degrees; cohesion, $c_b = 10$ kPa;
- Unit weight of rock (based on laboratory testing): $\gamma_r = 25$ kN/m^3; and
- Fully drained slope (based on piezometric measurements).

As shown in Figure 15-12(c), the applicable equation for a wedge without a tension crack is as follows:

$$FS = \frac{3}{(\gamma_r H)}(c_a X + c_b Y) + A \tan\phi_a + B \tan\phi_b \quad (15.6)$$

The values for the factors X, Y, A, and B are determined from a number of angular relationships measured on a stereographic projection as illustrated in Figure 15-14. The computations are shown in the box on the next page.

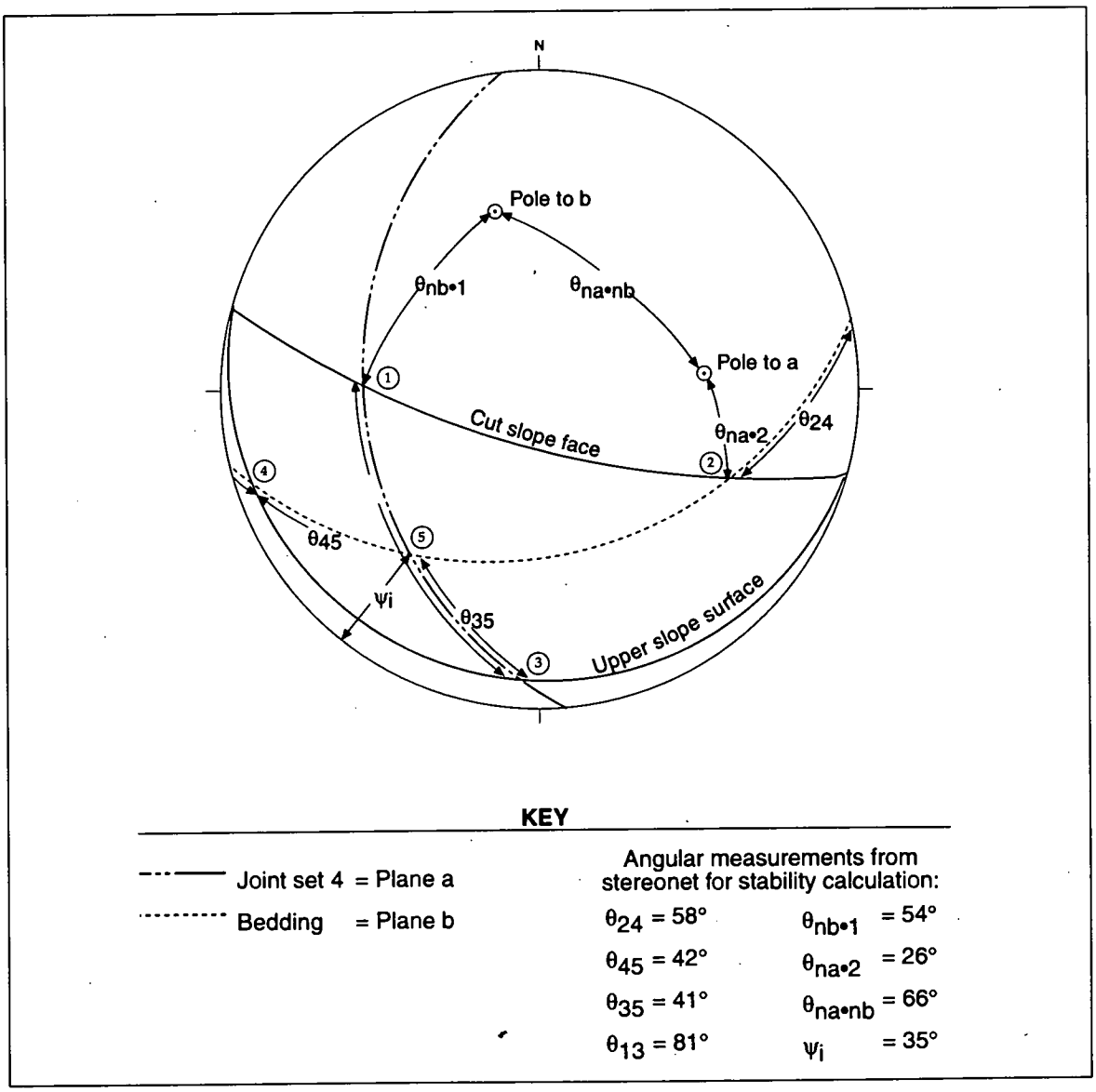

FIGURE 15-14 Angular measurements required for stability calculation for case example of wedge failure.

FIGURE 15-15 Primary toppling modes (Hoek and Bray 1981).

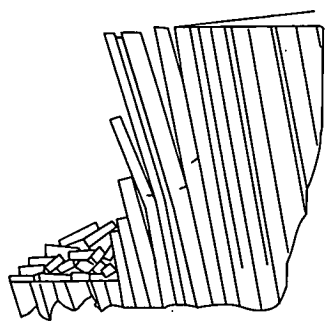

Flexural toppling in hard rock slopes with well developed steeply dipping discontinuities.

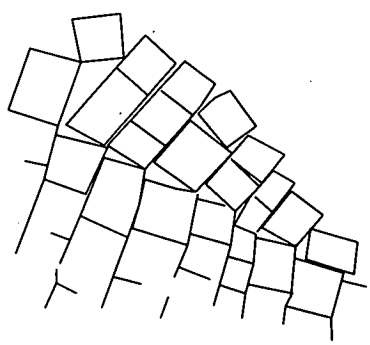

Block toppling in a hard rock mass with widely spaced orthogonal joints

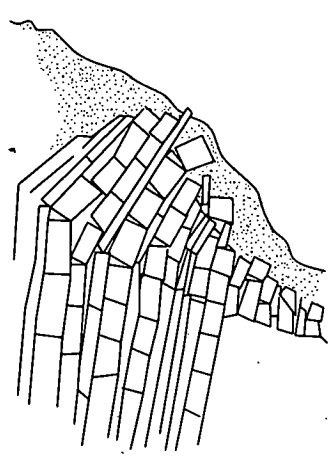

Block-flexure toppling characterized by pseudo-continuous flexure of long columns by accumulated motions along numerous cross joints.

$$X = \frac{(\sin\theta_{24})}{(\sin\theta_{45}\cos\theta_{(na2)})} = \frac{(\sin 58°)}{(\sin 42° \cos 26°)} = 1.41$$

$$Y = \frac{(\sin\theta_{13})}{(\sin\theta_{35}\cos\theta_{(nb1)})} = \frac{(\sin 81°)}{(\sin 41° \cos 54°)} = 2.56$$

$$A = \frac{[\cos\Psi_a - \cos\Psi_b \cos\theta_{(na \cdot nb)}]}{[\sin\Psi_5 \sin^2\theta_{(na \cdot nb)}]}$$

$$= \frac{(\cos 45° - \cos 48° \cos 66°)}{(\sin 35° \sin^2 66°)} = 0.91$$

$$B = \frac{[\cos\Psi_b - \cos\Psi_a \cos\theta_{(na \cdot nb)}]}{[\sin\psi_5 \sin^2\theta_{(na \cdot nb)}]}$$

$$= \frac{(\cos 48° - \cos 45° \cos 66°)}{(\sin 35° \sin^2 66°)} = 0.80$$

Substituting these values into Equation 15.6 gives

$$FS = \frac{\{3[(20)(1.41) + (10)(2.56)]\}}{[(25)(30)]} + (0.91)\tan 35° + (0.80)\tan 25°$$

$$FS = 0.22 + 0.64 + 0.37 = 1.23$$

This computed factor of safety is at the lower bound for most geotechnical engineering practice, and consideration should be given to reinforcement of the slope with tensioned rock anchors (see Chapter 18).

If poor blasting practices were utilized in the excavation process, it is possible that the cohesion along the discontinuities could have been destroyed. In this case, the first term of Equation 15.6 would be zero and the resultant factor of safety would be equal to 1.01. The wedge would probably fail during excavation; this analysis illustrates the importance of carefully controlled blasting in the creation of stable permanent slopes (see Chapter 18).

6. TOPPLING FAILURE

Toppling failures most commonly occur in rock masses that are subdivided into a series of slabs or columns formed by a set of fractures that strike approximately parallel to the slope face and dip steeply into the face [Figure 15-1(c)]. In a toppling failure the rock column or slab rotates about an essentially fixed point at or near the base of the slope at the same time that slippage occurs between the layers. A rarer case of toppling is that of a single column defined by a unique discontinuity such as a fault.

Rock types most susceptible to this mode of failure are columnar basalts and sedimentary and metamorphic rocks with well-developed bedding or foliation planes [Figure 15-1(*c*)]. As described by Hoek and Bray (1981), there are several types of toppling failures, including flexural, block, or a combination of block and flexural toppling (Figure 15-15). Toppling can also occur as a secondary failure mode associated with other failure mechanisms such as block sliding. Examples of these various types of secondary toppling failure are shown in Figure 15-16.

In order for toppling to occur, the center of gravity of the column or slab must fall outside the dimension of its base. Toppling failures are characterized by significant horizontal movements at

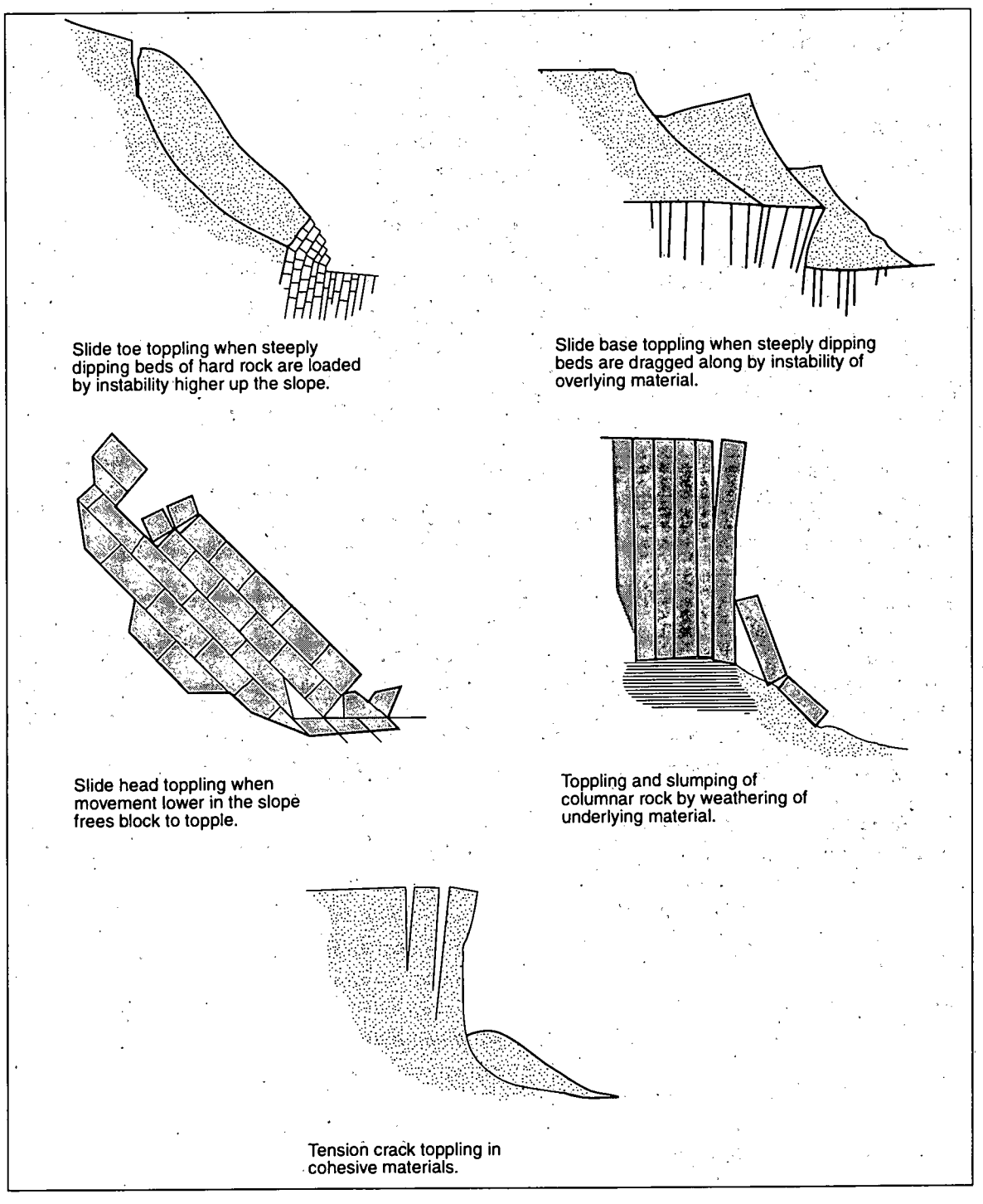

FIGURE 15-16 Secondary toppling modes (Hoek and Bray 1981).

the crest and very little movement at the toe. To accommodate this differential movement between the toe and crest, interlayer movement must occur. Thus, shear strength between layers is crucial to the stability of a slope that is structurally susceptible to toppling. Another characteristic of toppling movements is the antecedent development of major tension cracks behind the crest and parallel to the strike of the layers. Failure does not occur until there is shear failure of the slabs at the base of the slope. Slopes with rock structure that is susceptible to toppling can be induced to fail by increased pore-water pressures or by erosion or excavation at the toe of the slope.

6.1 Kinematic Analysis

Figure 15-17 indicates the slope parameters that define an analytical model for toppling analysis and the kinematic analysis of toppling using stereonet projection. The slope parameters necessary for analysis of Goodman and Bray's (1976) model of toppling failures are defined in Figure 15-17(*a*). Of particular note is the presence of a stepped failure base assumed to develop along cross fractures between the columns. The necessary conditions for toppling failure can be summarized as follows:

1. The strike of the layers must be approximately parallel to the slope face. Differences in these orientations of between 15 and 30 degrees have been quoted by various workers, but for consistency with other modes of failure, a value of 20 degrees seems appropriate.
2. The dip of the layers must be into the slope face. Using the dip direction convention, conditions 1 and 2 can be stated as follows: the dip direction of the layers must be between 160 and 200 degrees to the dip direction of the slope face.
3. As stated by Goodman (1980), in order for interlayer slip to occur, the normal to the toppling plane must have a plunge less than the inclination of the slope face less the friction angle of the surface. This condition can be formulated as follows:

$$(90° - \Psi_p) \leq (\Psi_f - \phi_p) \qquad (15.7)$$

where

Ψ_p = dip of geologic layers (planes),
Ψ_f = dip of slope face, and
ϕ_p = friction angle along planes.

On the basis of extensive development of nomograms for analysis of toppling, Choquet and Tanon (1985) proposed the following modification to this kinematic condition:

$$(90° - \Psi_p) \leq (\Psi_f - \phi_p + k) \qquad (15.8)$$

where $k = 0$ for $\phi_p < 20$ degrees and $k = 3/5(\phi_p - 20$ degrees) for $\phi_p \geq 20$ degrees.

Analogous to planar failures, some limitation to the lateral extent of the toppling failure is a fourth condition for a kinematically possible failure. Because the analysis is two-dimensional, it is usually assumed that zero-strength lateral release surfaces are present or that the potential failure mass is defined by a convex slope in plan.

6.2 Stability Analysis

The analysis of toppling failures has been investigated by several researchers, including Goodman and Bray (1976), Hittinger (1978), and Choquet and Tanon (1985). The analytical procedures are not as clearcut as for other methods of rock slope failure, particularly the concept of factor of safety. In general terms, the techniques check that the center of gravity for a specific column of rock lies within the base area of that column. Columns in which the center of gravity lies outside the base are susceptible to toppling.

The method developed by Goodman and Bray (1976) considers each column in turn proceeding from the crest of the slope to the toe and determines one of three stability conditions: stable, plane sliding, or toppling. The stability condition depends on the geometry of the block, the shear strength parameters along the base and on the sides of the column, and any external forces. Those columns that are susceptible to either sliding or toppling exert a force on the adjacent column in the downslope direction. The analysis is carried out for each column in the slope section so that all the intercolumnar forces are determined. The stability of the slope generally cannot be explicitly stated in terms of a factor of safety. However, the ratio between the friction value required for limiting equilibrium and that available along the base of the columns is often used as a factor of safety for toppling analyses. Figure 15-18 demonstrates the method of analysis for a toppling failure. The reader is referred to Hoek and Bray (1981) for a more comprehensive summary

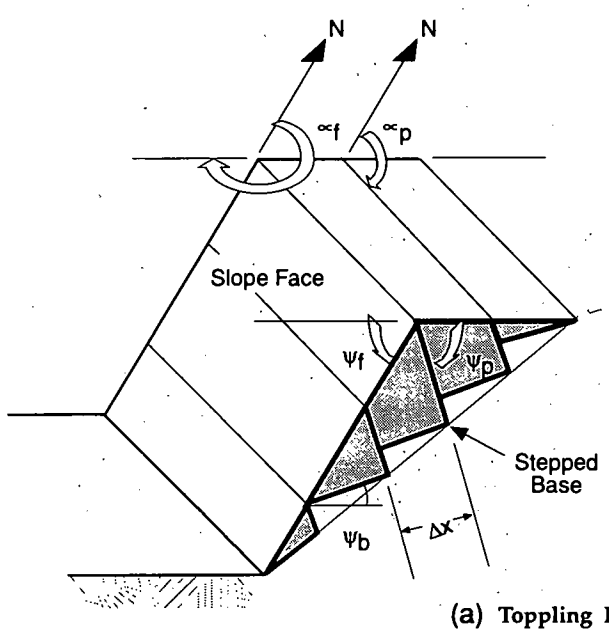

KEY:
$\propto_f$ = face dip direction
$\propto p$ = plane dip direction
ψb = base dip
ψ_f = face dip
ψ_p = plane dip
ϕ_b = base friction angle
ϕ_p = plane friction angle
Δx = width of columns

CONDITIONS FOR TOPPLING FAILURE
1. $\propto_p = (\propto_f \pm 180°) \pm 20°$
2. $(90° - \psi_p) \leq (\psi_f - \phi_p)$

(a) **Toppling Failure Model**

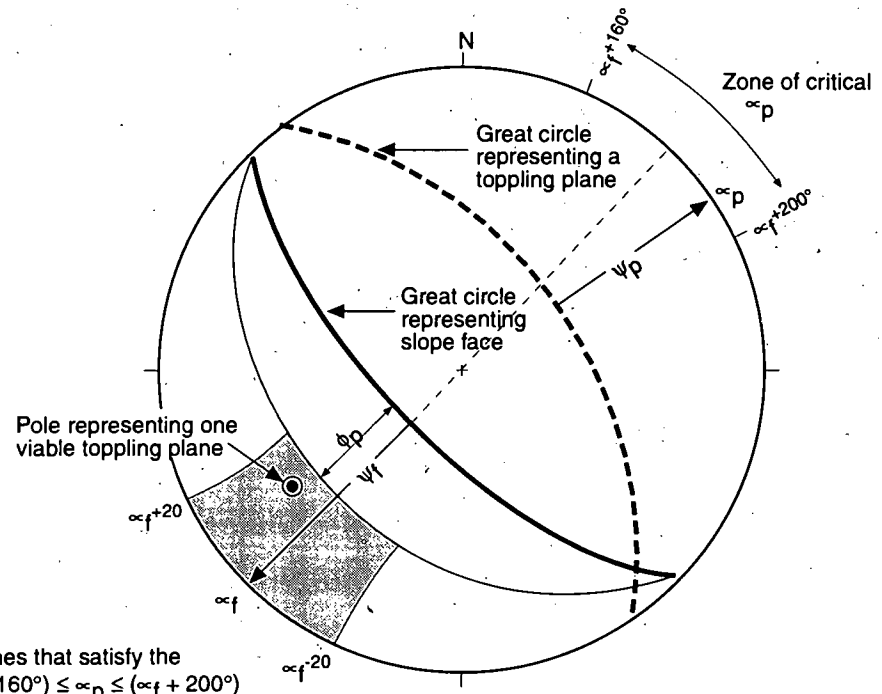

Discontinuity planes that satisfy the inequalities $(\propto_f + 160°) \leq \propto_p \leq (\propto_f + 200°)$ and $(90° - \psi_p) \leq (\psi_f - \phi_p)$ are kinematically viable toppling planes. The poles of such planes plot within the shaded area.

(b) **Great Circle Representation**

FIGURE 15-17
Kinematic analysis for toppling failure.

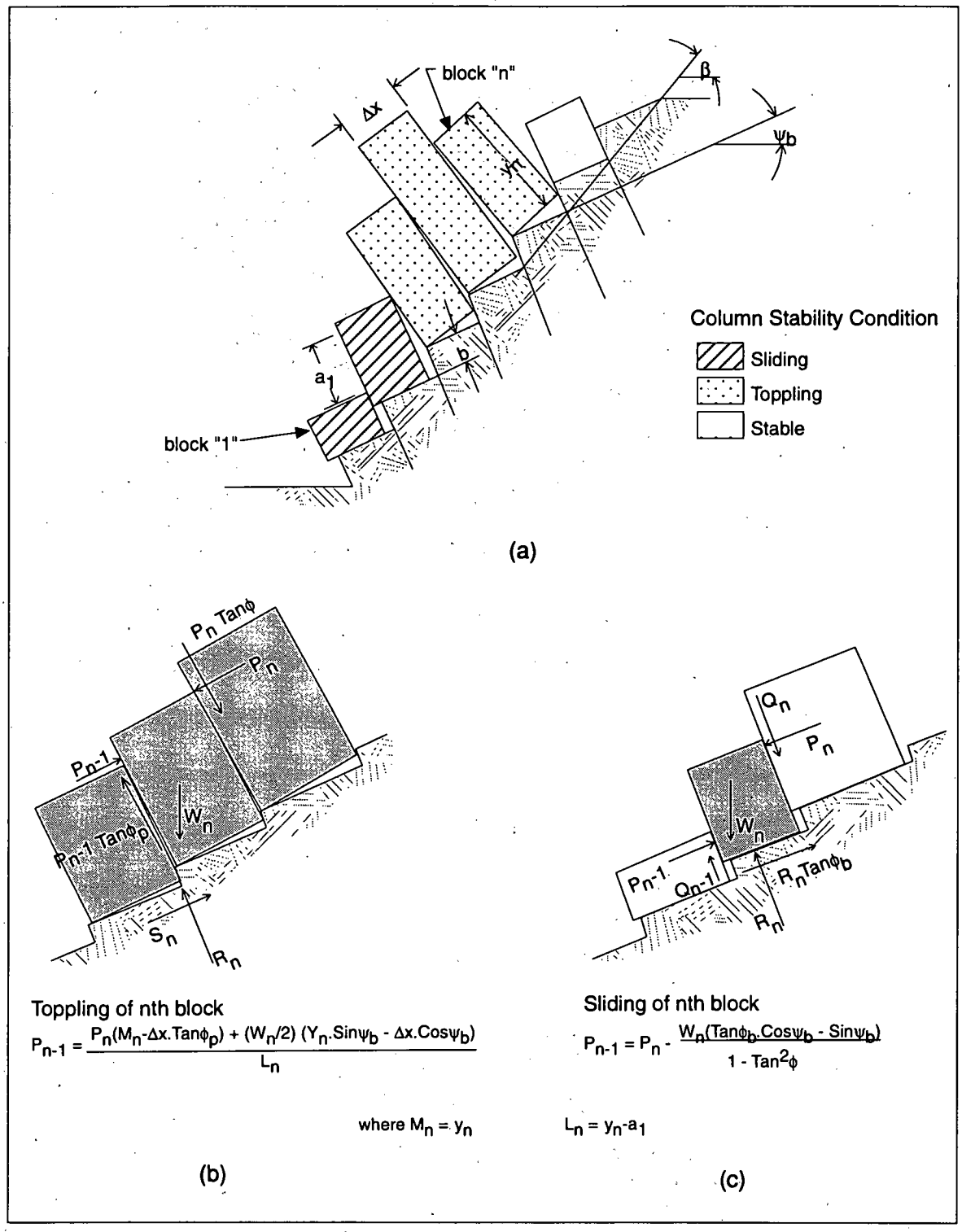

FIGURE 15-18
Stability equations for toppling failure (Hoek and Bray 1981).

of this technique or to Hittinger (1978) for a computer solution of toppling analyses. Wyllie (1992) has expanded this analysis to include external loads and water pressures.

Choquet and Tanon (1985) utilized the computer solution developed by Hittinger (1978) to derive a series of nomograms for the assessment of toppling failures. Unique nomograms were developed based upon the interlayer angle of shearing resistance, ϕ_p. A nomogram for ϕ_p = 30 degrees is given in Figure 15-19(*a*). Inherent in these nomograms are the following assumptions:

1. The columns in the model have a constant width, defined as Δx [Figure 15-17(*a*)].
2. The base of each column forms a stepped failure base with an inclination assumed at +15 degrees [Ψ_b = 15 degrees in Figure 15-17(*a*)].
3. No pore-water pressures are present within the slope.

An example of the use of this method of analysis is illustrated in Figure 15-19. Note that the formulation yields the limiting column width, Δxe, at which toppling failure occurs. The input variables for the example are

Friction angle for plane = ϕ_p = 30 degrees,
Dip of face = Ψ_f = 64 degrees,
Dip of plane = Ψ_p = 60 degrees.

From Figure 15-19(*a*), the ratio of $H/\Delta xe$ is 10 at the onset of toppling or limiting equilibrium (see the point indicated by the star). Thus, for a slope height of H = 20 m, Δxe = 2 m. If the column width is less than 2 m, the slope will be unstable with respect to toppling. This result is illustrated in Figure 15-19(*b*). Similarly, for a slope height of H = 10 m, the limiting column width would be 1 m.

Choquet and Tanon (1985) suggested that the factor of safety be evaluated by the ratio of the actual column width, Δx, to the theoretical limiting column width, Δxe, according to

$$FS = \frac{(\Delta x)}{(\Delta xe)} \tag{15.9}$$

where for $FS > 1$, the slope is stable against toppling and for $FS < 1$, the slope is unstable against toppling.

Figure 15-19(*c*) shows a sensitivity curve for the dip of the slope face, Ψ_f, as a function of the limiting column width, Δxe, for a constant dip of plane, Ψ_p = 60 degrees, and slope height H = 15 m. This curve is developed from the nomogram in Figure 15-19(*a*) by determining the corresponding $H/\Delta xe$ values for each of the Ψ_f curves. The sensitivity curve demonstrates that a slope with a face angle of 67 degrees has a limiting column width of 2 m. If the actual width is greater than this value, the slope will be stable against toppling, and conversely if it is less, the slope will be unstable. By comparison, if the actual column width was 4 m, the slope would be stable at a face angle of 82 degrees.

Stabilization of toppling failures can be accomplished by reducing the aspect ratio of the columns in one of two ways: by reducing the slope height so that column height is reduced or by bolting layers together to increase the base width of the columns. Both of these methods change the column geometry so that the centers of gravity of the columns are within their bases.

7. CIRCULAR FAILURE

For the purposes of this discussion, a circular failure is defined as a failure in rock for which the failure surface is not predominantly controlled by structural discontinuities and that often approximates the arc of a circle [Figure 15-1(*d*)]. It should be recognized that there is a complete spectrum of structural control of rock failures ranging from completely structurally controlled, to those that are in part structurally controlled and in part material failures, to those in which structure has little or no influence. Rock types that are susceptible to circular failures include those that are partially to highly weathered and those that are closely and randomly fractured. In either case the rock mass is so highly fragmented that the failure surface can avoid passing through the stronger intact rock material. In this sense, a circular failure in rock can be considered much like that through a soil mass with a very large grain size.

The characteristics of circular failure in rock are similar to those for a classical rotational failure in soil except that the failure surface in rock tends to form a shallow, large-radius circle. Figure 15-1(*d*) illustrates an example of such a failure in a highly weathered basalt. Slope movement at the crest of the slope tends to be very steep, whereas movement at the toe tends to be subhorizontal. In general, signs of slope distress precede a rotational

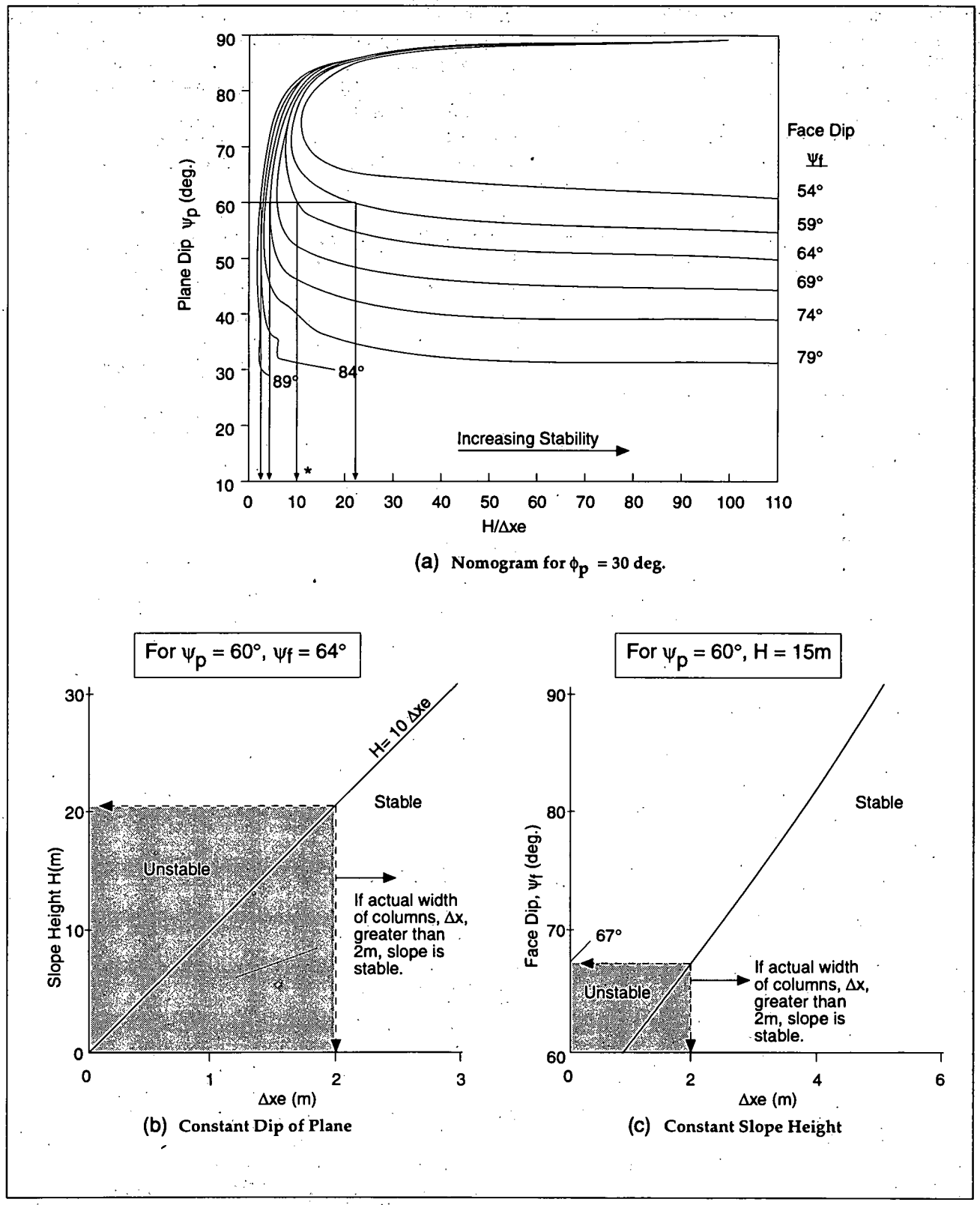

FIGURE 15-19
Nomogram analysis of toppling stability (Choquet and Tanon 1985).
REPRINTED FROM ASHWORTH, E. (ED.), RESEARCH AND ENGINEERING APPLICATIONS IN ROCK MASSES, *26TH U.S. SYMPOSIUM ON ROCK MECHANICS*, 26–28 JUNE 1985, SOUTH DAKOTA SCHOOL OF MINES AND TECHNOLOGY, RAPID CITY, 1985, 1340 PP., 2 VOLUMES, A.A. BALKEMA, OLD POST ROAD, BROOKFIELD, VERMONT 05036

failure in rock. These signs of distress include arcuate tension cracks near the crest of the slope, bulging in the toe area of the slide, and longitudinal cracks parallel to the inclination of the slope face. Before failure there usually is a period of accelerating movement, which generally can be monitored in order to predict failure.

7.1 Kinematic Analysis

The kinematic analysis for the circular mode of failure is in reality an analysis to exclude other modes of structurally controlled failure that have been discussed in the foregoing sections. In general, the structural discontinuities do not form distinct patterns and the dominant structures are not oriented with respect to the proposed slope configuration to develop a kinematically possible failure mode. An example of the latter case is the instance of a sedimentary sequence in which the bedding planes dip into the slope. Assuming that no other persistent structures are present, a circular failure model with appropriate allocation of rock-mass strength parameters would be suitable for slope design.

7.2 Stability Analysis

Appropriate methods of analysis for a circular failure in rock depend upon the shear-strength criterion used to characterize the rock-mass material. If the rock mass is assumed to obey the Mohr-Coulomb criterion, any of the analytical techniques developed for soil can be applied. These include stability charts as presented by Duncan (see Chapter 13) and Hoek and Bray (1981) and analytical techniques such as those presented by Janbu (1954), Bishop (1955), Morgenstern and Price (1965), and Sarma (1979). Details of the methodology for applying these various analytical techniques are considered in Chapter 13.

Because of the strong intact strength of the individual blocks and the high degree of interlock inherent in rock masses, it is more often the case that the material is very dilatant as it is sheared. For this reason, many investigators have found it appropriate to characterize the rock mass with a nonlinear shear-strength criterion. Several criteria have been proposed, including those by Landanyi and Archambault (1970) and by Hoek and Brown (1980). If criteria such as these are utilized, an analytical method similar to that presented in Chapter 14 must incorporate the ability to determine shear strength as a function of normal stress for each slice along the failure surface.

Several workers have presented useful failure charts for the rapid solution of simplified stability problems involving the circular failure mechanism. Each specific chart is applicable to a particular location of the phreatic surface ranging from fully drained to fully saturated. The solutions vary in technique but generally involve the calculation of one or more dimensionless ratios. These values in combination with the slope angle graphically determine corresponding dimensionless ratios from which the factor of safety can be calculated. The reader should refer to Chapter 13 for examples of stability charts for circular failures.

Such stability charts are very useful in rapidly carrying out sensitivity analyses of any of the parameters affecting stability and are also used to back analyze circular slope failures. Typical limitations of such charts include the following:

- A single material type is present throughout the slope,
- The slope inclination is uniform or can be approximated by a single value,
- The upper slope surface is horizontal,
- Pore-water pressures can be treated as a simple phreatic surface (i.e., there is no capability for modeling piezometric surfaces),
- The critical circle is assumed to exit through the toe of the slope or to be bounded by a firm base layer, and
- External loads such as earthquakes or reinforcement cannot be incorporated.

To analyze stability problems where conditions may preclude the use of stability charts generally requires the utilization of a computer program such as XSTABL (Sharma 1994), PC-STABL5 (Carpenter 1986), and LISA (Hammond et al. 1990), and the method developed by Sarma (1979) and adapted by Hoek (1986). The Sarma program is particularly useful because it allows the slope to be subdivided into slices, the boundaries of which can correspond to known geologic structures (i.e., slice boundaries are not constrained to be vertical). The Sarma program also allows distinct strength parameters to be applied to each segment of the sliding surface and to each slice boundary. This program is amenable to analyses with nonlinear shear strength criteria because it allows the user to determine the

interslice stresses and to assign appropriate apparent friction and apparent cohesion values from the failure envelope. For examples of this type of analysis, the reader is referred to McCreath (1991) and Wyllie (1992, Chapter 6).

8. OTHER FAILURE MODES AND ANALYTICAL TECHNIQUES

The preceding sections have dealt with the four most common methods of stability analysis for rock slopes. Two additional failure modes that require specific structural fabric are column buckling and the bilinear wedge. For completeness, these failure modes are described next. The balance of this section deals with the issue of slope design under dynamic loading and with specialized analytical techniques based on probabilistic and distinct-element methods.

8.1 Column Buckling Failure

Slopes that contain steeply dipping repetitive discontinuities, such as bedding surfaces that parallel the slope face, may be susceptible to column buckling. Such a slope face is often referred to as a *dip slope*. The failure mode involves planar movement along the discontinuity and a material failure near the toe of the slope by buckling (Figure 15-20).

The necessary structural conditions that cause this failure mode to be kinematically feasible are similar to those for planar failure with the exception that the discontinuity forming the failure surface does not daylight the slope face but is parallel to it. As with the toppling failure mode, buckling failure is most probable in rocks with thin slabs.

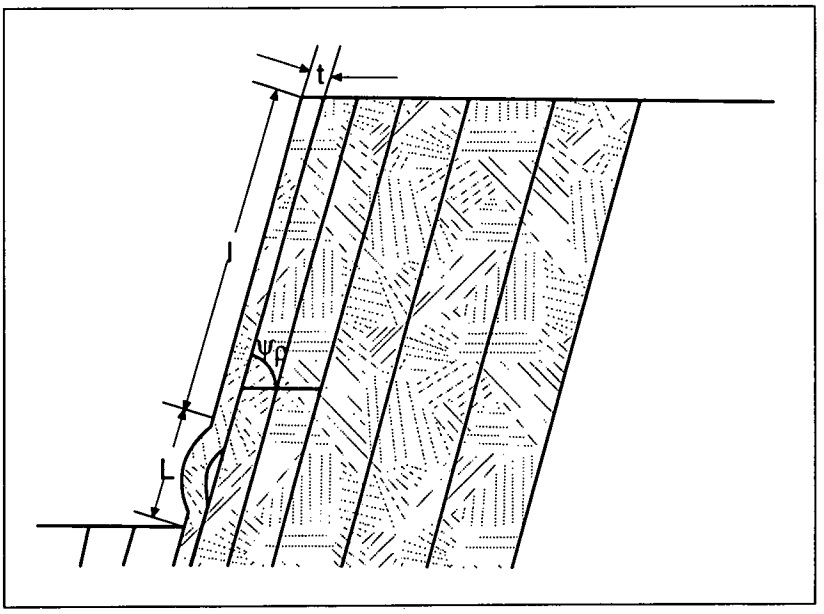

FIGURE 15-20 Column buckling failure mode (modified from Goodman 1980).

This mode of failure is typically analyzed using the classical methods for column stability in which the stress parallel to the axis of a column is equal to Euler's critical stress for buckling (Goodman 1980; Cavers 1981). Parameters in the analysis include the length, l, and thickness, t, of the column; the length of the buckling zone, L; the inclination of the columns, Ψ_p; the shear strength along the columns; and the compressive rock strength (Figure 15-20). Buckling failures have occurred in high-footwall mine slopes in coal-measure sequences. Slopes that have experienced this type of failure are usually more than 200 m high. Only under unusual circumstances involving high-dip slopes in thinly bedded weak rock does buckling failure represent a design consideration for slopes along transportation corridors.

8.2 Bilinear Wedge Failure

In some situations a combination of discontinuities may define a failure mass composed of two blocks as shown in Figure 15-21. The upper active block is separated from the lower passive block by steeply dipping discontinuities that allow interblock movements to occur. The failure surface is usually defined by major planar structures such as faults. The upper block is unstable and exerts a force on the passive block.

The kinematic conditions for the two structures that form the bilinear failure surface are similar to those previously discussed for planar failure. The dip of the upper plane must exceed its angle of friction, and the dip of the lower plane must be less than the angle of friction for that surface. Although the most common configuration of this failure mode is for the lower failure surface to have a dip toward the slope face, a case has been reported by Calder and Blackwell (1980) in which the lower plane dipped into the slope. Survey monitoring demonstrated that at this site, movement of the passive block actually included an upward component.

The unique kinematic condition for this failure mode is that a geologic structure must be present that will allow differential movement between the blocks. At the intersection of the active and pas-

sive blocks on the failure surface, movements probably result in local rock crushing so that a failure arc develops between the two planar segments of the failure surface.

With reference to Figure 15-21, the stability of a bilinear wedge is evaluated by calculating the resultant force, *R3*, which is transferred from the active block to the passive block across Plane 3. The force *R3* is the minimum to just resist sliding along Plane 1. The factor of safety is calculated by resolving the following forces:

- Resultant force, *R3*;
- Weight of the passive block, *Wp*;
- Shear force, *R2*; and
- Any uplift or driving forces due to water pressures along Plane 2.

The factor of safety of the bilinear wedge is the ratio of the total resisting force to the total driving force along this plane (CANMET 1977).

This type of failure is relatively uncommon; the reader is referred to the *Pit Slope Manual* (CANMET 1977) and *Introduction to Rock Mechanics* (Goodman 1980) for more detailed discussions.

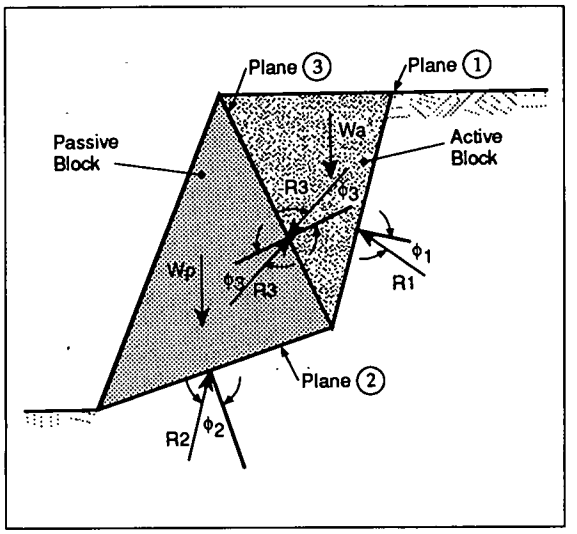

FIGURE 15-21 Bilinear failure mode (modified from CANMET 1977).

8.3 Analysis of Earthquake Effects on Rock Slope Stability

Dynamic forces introduced in rock slopes should be considered in slope design analyses for areas susceptible to earthquakes. Design accelerations for a particular site are estimated from consideration of the Maximum Credible Earthquake (MCE) along each fault in the vicinity of the site. For each MCE and fault combination, distance-attenuation relationships are used to develop the resultant acceleration, expressed as a fraction of gravitational acceleration, for the site. The critical MCE-fault combination produces the highest or design acceleration for the site. In critical situations design accelerations can be developed using such seismological techniques. In most cases, seismic zoning maps provide adequate baseline data for design accelerations.

Pseudostatic analysis and Newmark analysis (Newmark 1965) are two commonly used engineering design methods that incorporate the forces due to earthquakes. In theory these methods can be applied to all the failure mechanisms for rock slopes previously discussed.

8.3.1 Pseudostatic Analysis

In the pseudostatic method, a force is applied to the unstable block equal to the product of the design acceleration and the weight of the block. This force is usually applied horizontally so as to decrease stability (Case i, Figure 15-22). Other investigators (e.g., Mayes et al. 1981) have suggested that the earthquake force be applied in two components, a horizontal component due to the design acceleration and a vertical component acting in an upward direction and equal to two-thirds of the horizontal component. The resultant force is 1.2 times the horizontal force and acts in a direction 34 degrees above the horizontal (Case ii, Figure 15-22). The latter formulation is obviously more conservative than the former.

Although the pseudostatic method is the most common way to include forces due to earthquakes in stability calculations, the method is inherently conservative because the cyclic loading due to the earthquake is replaced by a constant force equal to the maximum transient force. This conservatism is accounted for in the analyses by designing for a factor of safety that is lower for the pseudostatic analysis than for the static analysis. For example, whereas an acceptable static factor of safety for a rock slope may be 1.25 to 1.5, an acceptable factor of safety under pseudostatic conditions may be 1.0 to 1.1.

8.3.2 Newmark Analysis

Newmark's method (Newmark 1965) predicts the displacement of the slope under an acceleration-

FIGURE 15-22
Pseudostatic analysis.

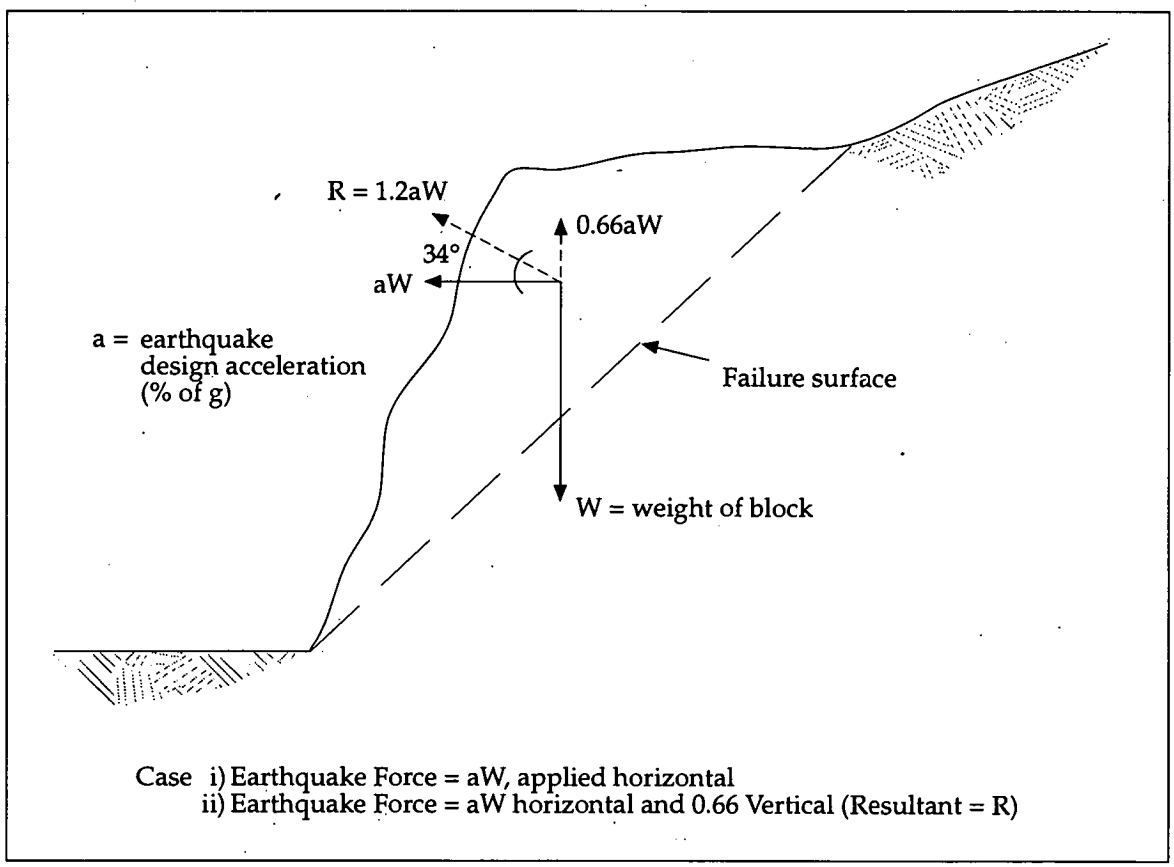

time record appropriate for the site. In the first step of the analysis, permanent displacement of the slope is assumed to occur only when the earthquake acceleration exceeds the critical acceleration for the geometry and preexisting stability condition of the slope (Jibson 1993). The cumulative permanent displacement of the slope is the sum of those portions of the acceleration-time history that exceed the critical acceleration value (Figure 15-23).

$$a_c = (FS - 1)g \sin\Psi_p \qquad (15.10)$$

where

a_c = critical acceleration,
g = acceleration due to earth's gravity,
FS = static factor of safety, and
Ψ_p = angle from the horizontal that the center of mass of the slide first moves (equal to inclination of failure plane).

Thus a slope with a static FS close to unity has a critical acceleration close to zero and experiences movement under any earthquake motion.

The second step in the Newmark analysis is to calculate the displacement for the ground motion record selected for the site by double integration of those portions of the record that lie above the critical acceleration, as shown in Figure 15-23. Jibson (1993) has presented both rigorous and simplified methods to calculate the Newmark displacement.

Interpretation of the results of a Newmark analysis requires knowledge of the relationship between shear strength and shear strain for the material along the failure surface. Materials that show ductile behavior may accommodate the calculated displacement with little effect, whereas in brittle materials the displacement may lead to rapid strength loss and failure. For most rock slope design situations, and particularly for reinforced rock slopes, the strength-strain relationship is unknown and the Newmark method is difficult to apply.

8.4 Probabilistic Analysis

General engineering design practice has evolved the concept of factor of safety to determine the margin of conservatism that should be explicitly incorporated into a design. Typical factor-of-safety values used in geotechnical engineering

practice for static design in transportation projects are as follows:

Slopes with potential impact on permanent structures: $FS = 1.5$ to 2.0;
Slopes with no potential impact on permanent structures: $FS = 1.25$ to 1.5.

The factor-of-safety concept is appropriate where material properties can be specified and stresses accurately computed. In geotechnical engineering these requisites are not generally present. It is often necessary to perform a testing or field measurement program of limited scope and to use engineering judgment to assign so-called "design values." Because the design analysis incorporates many such variables, each with its own degree of uncertainty, the cumulative impact upon the calculated factor of safety is difficult to assess.

An alternative approach that is beginning to gain broad acceptance is an index to the factor of safety referred to as the *coefficient of reliability* or alternatively as the *probability of failure*. These indexes are expressed as a decimal fraction of unity, and their sum is 1.0. Although either can be used in probabilistic analysis, the adoption of one over the other is an issue of perception. Not surprisingly, the former is more readily accepted by property owners than is the latter.

In this analysis process, the uncertainty in each variable is incorporated into the analytical process by assigning a probability distribution function (PDF) to each variable instead of a single design value. For example, multiple measurements of the angle of friction of a joint surface may yield a mean value of 32 degrees with a standard deviation of 5 degrees. This mean value can be incorporated into the probabilistic analysis as a normal distribution with the stated parameters. The range of all the variables in the analysis can be similarly defined by PDFs, although the type of distribution can be triangular, normal, lognormal, beta, or other (Wyllie 1992). For example, PDFs can be assigned to water levels, discontinuity inclination, unit weight, and cohesion.

The analysis requires selection of a value from each of the PDFs on a random basis and then calculation of a factor of safety. Typically, a Monte Carlo simulation is used to generate random numbers from which each of the variable values is assigned. By repeating this process a large number of times (100 or more), a cumulative distribution function (CDF) for the factor of safety can be developed. An example of this process is shown in Figure 15-24. As a result of such an analysis, the slope practitioner is in a position to state that the coefficient of reliability is x percent (or that the probability of failure is $100 - x$ percent). This probability of failure can be evaluated in conjunction with the consequences of failure to determine an optimum course of action. In cases where all of the consequences of failure can be expressed in monetary terms, the optimum course of action will be the one that is most cost-effective. Applications of this methodology to transportation corridors have been described by Wyllie et al. (1979) and Roberds (1990, 1991) and an illustrative application to an open pit mine slope by Piteau and Martin (1977).

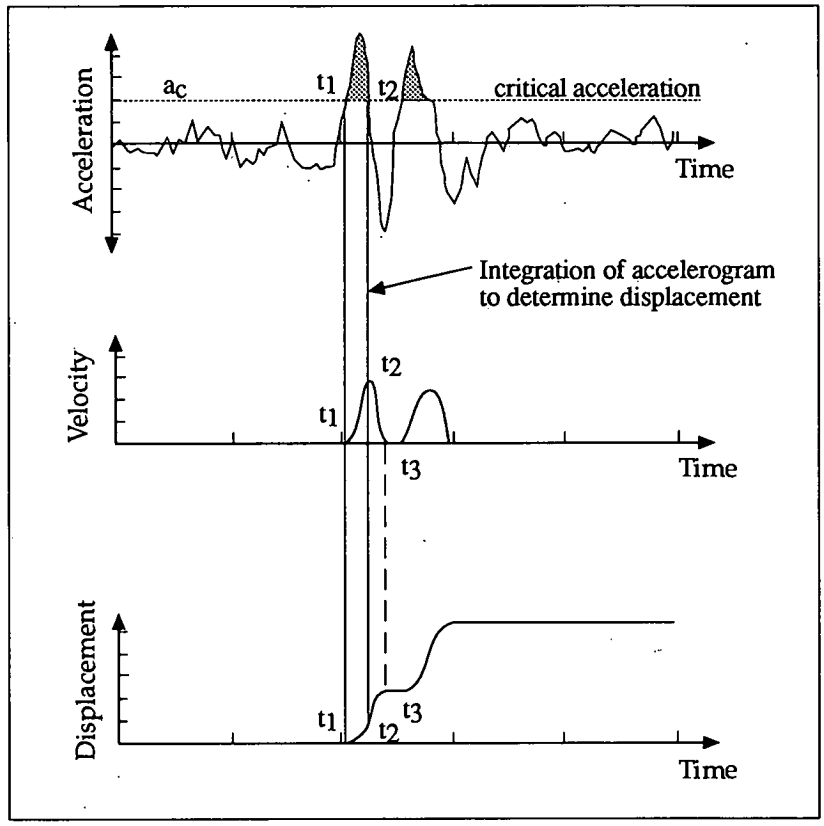

FIGURE 15-23 Newmark analysis (Jibson 1993).

8.5 Three-Dimensional Analyses

Two-dimensional analyses evaluate geometric, material, and loading conditions along a vertical section aligned normal to the slope. Thus, lateral forces are not considered. In most cases the analysis of a unit thickness of the slope provides an acceptable factor of safety. Three-dimensional

FIGURE 15-24 Probabilistic slope stability analysis.

INPUT

Consider Equation 15-4 for planar failure:

$$FS = \frac{(cA + W\cos\Psi_p \tan\phi)}{(W\sin\Psi_p)}$$

Stochastic Variables: (cumulative probability distributions for each variable defined by testing or measurement and fitted to standard distribution type such as normal, log-normal etc.)

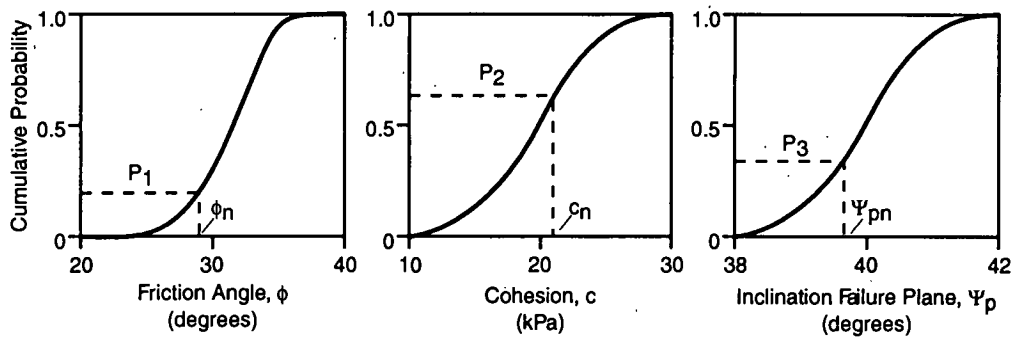

METHOD

Monte Carlo Analysis

1. *For the "nth" FS calculation:*

Generate random numbers P_1, P_2, P_3 between 0 and 1.

From distributions calculate ϕ_n, c_n, Ψ_{pn}.

Calculate FS_n

2. Repeat procedure until n = 100, 200, etc.

RESULT

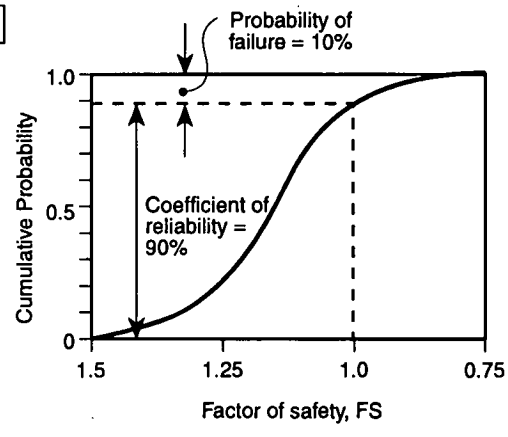

analyses may be warranted where the assumption of uniformity in the transverse direction cannot be made, for example, on slopes with sharp convex or concave curvatures in plan. Two-dimensional analyses of such configurations can either underestimate or overestimate the factor of safety.

Hungr et al. (1989) developed an application of Bishop's simplified method for three-dimensional limit-equilibrium analysis referred to as CLARA. The method subdivides the failure mass into a series of columns rather than slices as is the case in the two-dimensional formulation. The vertical intercolumnar shear forces are neglected in the analysis, which can lead to conservative results when applied to some asymmetrical failure masses in which the energy required to overcome internal deformation of the failure mass contributes to stability. However, for rotational or symmetrical sliding surfaces for which the internal strength can be neglected, the method is useful (Hungr et al. 1989). Hungr et al. (1989) also presented applications of the model to rotational, wedge, and bilinear sliding surfaces.

8.6 Distinct-Element Method

Methods of analysis other than limit equilibrium have been utilized to analyze slopes in which kinematically feasible failure modes are not present, yet observation and monitoring indicate that displacements are occurring. One such method is the distinct-element method described by Cundall (1987) and Lorig et al. (1991). This method does not require a prescribed failure surface in order to reach a solution. The iterative calculation procedure models the progressive failure of slopes, a process that generates a surface of demarcation between a group or groups of stable blocks and a group or groups of unstable blocks.

As stated by Lorig et al. (1991), the three attributes of the distinct-element method that distinguish it from other numerical methods are as follows:

1. The rock mass is composed of individual blocks that can undergo large rotation and large displacements relative to one another,
2. Interaction forces between blocks arise from changes in their relative geometrical configuration, and
3. The solution scheme is explicit in time.

The distinct-element method utilizes a calculation procedure that solves the equations of motion and contact force for each modeled rigid block at each time step [Figure 15-25(*a*)]. Block interaction at contact points is modeled by strength and deformation parameters. As shown in Figure 15-25(*b*), the analysis provides the sequential positions and velocities of each block and thus is useful when predictions of slope displacement are required. The method can also be used to incorporate reinforcing elements, to analyze foundation loading on rock, and to carry out dynamic analyses using earthquake velocity records. Computer programs have been formulated for both two-dimensional and three-dimensional distinct-element analyses.

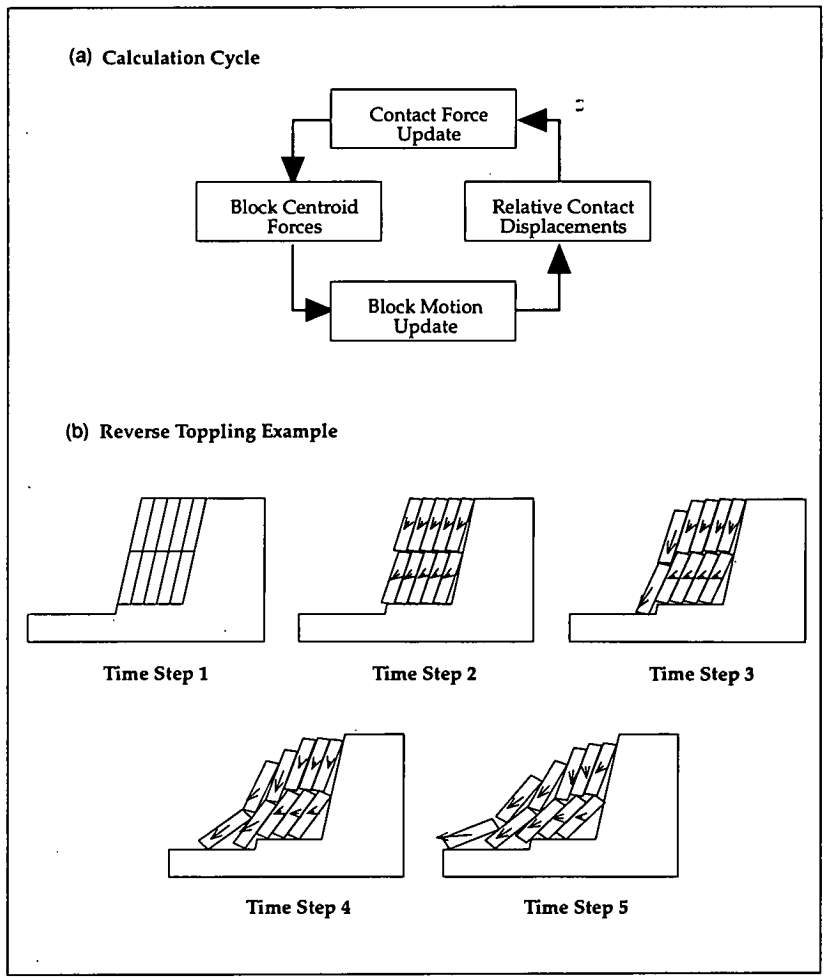

FIGURE 15-25 Distinct-element method (Lorig et al. 1991).

REFERENCES

Bishop, A.W. 1955. The Use of the Slip Circle in the Stability Analysis of Slopes. *Geotechnique*, Vol. 5, No. 1, pp. 7–17.

Calder, P.N., and G.H. Blackwell. 1980. Investigation of a Complex Rock Slope Displacement at Brenda Mines. *Canadian Institute of Mining Bulletin*, Vol. 73, No. 820, pp. 73–82.

CANMET. 1977. *Pit Slope Manual*, Supplement 5-1: *Plane Shear Analysis*. Canada Centre for Mineral and Energy Technology, Ottawa, Ontario, 307 pp.

Carpenter, J. R. 1986. *STABL5/PC STABL5 User Manual*. Joint Highway Research Project Report to Indiana Department of Highways. School of Civil Engineering, Purdue University, West Lafayette, Ind., 46 pp.

Cavers, D. S. 1981. Simple Methods to Analyze Buckling of Rock Slopes. *Rock Mechanics*, Vol. 14, No. 2, pp. 87–104.

Choquet, P., and D. D. B. Tanon. 1985. Nomograms for the Assessment of Toppling Failure in Rock Slopes. In *Proc., 26th U.S. Symposium on Rock Mechanics*, South Dakota School of Mines and Technology, June 26–28, 1985, Rapid City, S.D., A.A. Balkema, Rotterdam, Netherlands, Vol. 1, pp. 19–30.

Cundall, P. A. 1987. Distinct Element Models of Rock and Soil Structure. In *Analytical and Computational Methods in Engineering Rock Mechanics* (E. T. Brown, ed.), George Allen and Unwin, London, pp. 129–163.

Franklin, J. A., and M. B. Dusseault. 1989. *Rock Engineering*. McGraw-Hill, Inc., New York, 600 pp.

Goodman, R. E. 1976. *Methods of Geological Engineering in Discontinuous Rocks*. West Publishing Co., St. Paul, Minn., 472 pp.

Goodman, R. E. 1980. *Introduction to Rock Mechanics*. John Wiley & Sons, New York, 478 pp.

Goodman, R. E., and J. W. Bray. 1976. Toppling of Rock Slopes. In *Proc., Specialty Conference on Rock Engineering for Foundations and Slopes*, Boulder, Colo., American Society of Civil Engineers, New York, Vol. 2, pp. 201–234.

Hammond, C. J., S. Miller, D. Hall, and P. Swetik. 1990. *Level I Stability Analysis (LISA) User's Manual to Version 2.0*. Forest Service, U.S. Department of Agriculture, Ogden, Utah, 256 pp.

Hittinger, M. 1978. *Numerical Analysis of Toppling Failures in Jointed Rock Masses*. Ph.D. thesis. University of California, Berkeley, 297 pp.

Hodge, R. A. L., and R. A. Freeze. 1977. Groundwater Flow Systems and Slope Stability. *Canadian Geotechnical Journal*, Vol. 14, pp. 466–476.

Hoek, E. 1986. General Two-Dimensional Slope Stability Analysis. In *Analytical and Numerical Methods in Rock Engineering* (E. T. Brown, ed.), George Allen and Unwin, London, pp. 95–128.

Hoek, E., and J. W. Bray. 1981. *Rock Slope Engineering*, 3rd ed. Institution of Mining and Metallurgy, London, 402 pp.

Hoek, E., and E. T. Brown. 1980. *Underground Excavations in Rock*. Institution of Mining and Metallurgy, London, 527 pp.

Hungr, O., F. M. Salgado, and P. M. Byrne. 1989. Evaluation of a Three-Dimensional Method of Slope Stability Analysis. *Canadian Geotechnical Journal*, Vol. 26, No. 4, pp. 679–686.

Janbu, N. 1954. Application of Composite Slip Circles for Stability Analysis. In *Proc., European Conference on Stability of Earth Slopes*, Stockholm, Statens Reproduktionsanstalt, Vol. 3, pp. 43–49.

Jibson, R. W. 1993. Predicting Earthquake-Induced Landslide Displacements Using Newmark's Sliding Block Analysis. In *Transportation Research Record 1411*, TRB, National Research Council, Washington, D.C., pp. 9–17.

Landanyi, B., and G. Archambault. 1970. Simulation of Shear Behaviour of a Jointed Rock Mass. In *Proc., 11th Symposium on Rock Mechanics*, American Institute of Mining Engineers, New York, pp. 105–125.

Lorig, L. J. , R. D. Hart, and P. A. Cundall. 1991. Slope Stability Analysis of Jointed Rock Using the Distinct Element Method. In *Transportation Research Record 1330*, TRB, National Research Council, Washington, D.C., pp. 1–9.

Lowell, S. M. 1990. The K M Mountain Landslide near Skamokawa, Washington. *Washington Geologic Newsletter*, Vol. 18, No. 4, pp. 3–7.

Mathews, W. H., and K. C. McTaggert. 1969. The Hope Landslide, British Columbia. *Proc., Geology Association of Canada*, Vol. 20, No. 65-B, pp. 65–76.

Mayes, R. L., R. L. Sharpe, and J. D. Cooper. 1981. Seismic Design Guidelines for Highway Bridges. In *Proc., 50th Annual Convention*, Structural Engineers Association of California, Coronado, pp. 93–112.

McCreath, D. 1991. Use of Nonlinear Strength Criteria in Stability Analyses of Bridge Foundation on Jointed Rock. In *Transportation Research Record 1330*, TRB, National Research Council, Washington, D.C., pp. 10–21.

Moore, H. L. 1986. Wedge Failures Along Tennessee Highways in the Appalachian Region: Their Occurrence and Correction. *Bulletin of the Association of Engineering Geologists*, Vol. 23, No. 4, pp. 441–460.

Morgenstern, N. R., and V. E. Price. 1965. The Analysis of the Stability of General Slip Surfaces. *Geotechnique*, Vol. 15, No. 1, pp. 79–93.

Newmark, N. M. 1965. Effects of Earthquakes on Dams and Embankments. *Geotechnique*, Vol. 15, No. 2, pp. 139–159.

Piteau, D. R. 1972. Engineering Geology Considerations and Approach in Assessing the Stability of Rock Slopes. *Bulletin of the Association of Engineering Geologists*, Vol. 9, No. 3, pp. 301–320.

Piteau, D. R., and D. C. Martin. 1977. Slope Stability Analysis and Design Based on Probability Techniques at Cassiar Mine. *Canadian Institute of Mining Bulletin*, Vol. 70, No. 779, pp. 139–150.

Piteau, D. R., and F. L. Peckover. 1978. Engineering of Rock Slopes. In *Special Report 176: Landslides: Analysis and Control* (R. L. Schuster and R. J. Krizek, eds.), TRB, National Research Council, Washington, D.C., pp. 192–234.

Roberds, W. J. 1990. Methods for Developing Defensible Subjective Probability Assessments. In *Transportation Research Record 1288*, TRB, National Research Council, Washington, D.C., pp. 183–190.

Roberds, W. J. 1991. Methodology for Optimizing Rock Slope Preventative Maintenance Programs. In *Proc., Geotechnical Engineering Congress*, Boulder, Colo., American Society of Civil Engineers, New York, pp. 634–645.

Sarma, S. K. 1979. Stability Analysis of Embankments and Slopes. *Journal of the Geotechnical Engineering Division*, ASCE, Vol. 105, No. GT12, pp. 1511–1524.

Sharma, S. 1994. *XSTABL, An Integrated Slope Stability Analysis Program for Personal Computers: Reference Manual Version 5*. Interactive Software Designs, Inc., Moscow, Idaho, 214 pp.

Wyllie, D. C. 1992. *Foundations on Rock*. Chapman & Hall, London, 333 pp.

Wyllie, D. C., N. R. McCammon, and W. L. Brumund. 1979. Planning of Slope Stabilization Programs Using Decision Analysis. In *Transportation Research Record 749*, TRB, National Research Council, Washington, D.C., pp. 34–39.